

A comparison of the relationship between ground-measured particulate matter and aerosol optical depth derived from both Sentinel-3a and AERONET.



Submitted in part fulfilment of the requirements of the degree of MSc by Research in Earth
Observation

Swansea University

2022

Copyright: The Author, Caitlin Jones, 2022

Distributed under the terms of a Creative Commons Attribution-NonCommercial-ShareAlike 4.0
International License (CC BY-NC-SA 4.0).

Declarations

This dissertation is my own work and is the result of my own independent study. It has not been submitted for any other part of my degree assessment at Swansea University nor has any element of it been submitted for a qualification or published externally. Any third-party involvement in this study is declared in the acknowledgements and all secondary sources of information have been acknowledged fully in footnotes and references. A bibliography of all literature used in the work has been provided.

This work has not previously been accepted in substance for any degree and is not being concurrently submitted in candidature for any degree.

Signed..........
Date.....11/04/2024.....


This thesis is the result of my own investigations, except where otherwise stated. Other sources are acknowledged by footnotes giving explicit references. A bibliography is appended.

Signed..........
Date..... 11/04/2024.....

I hereby give consent for my thesis, if accepted, to be available for electronic sharing

Signed..........
Date..... 11/04/2024.....

The University's ethical procedures have been followed and, where appropriate, that ethical approval has been granted.

Signed..........
Date.....11/04/2024.....

Acknowledgements

I would like to thank the team at Swansea University, namely my supervisor Peter North and the Department of Geography admin team. Also, to my mother, Johanne; to the rest of my family; to my flatmates. Thank you for supporting me throughout this stressful time, for pushing me to keep working, and for all the time and advice you've given me.

Contents

Declarations	2
Acknowledgements.....	3
Abstract.....	6
1. Introduction	7
1.1. Motivation	7
1.2. Aerosol Measurements and Distribution	8
1.2.1. Particulate Matter.....	8
1.2.2. Aerosol Optical Depth.....	9
1.3. Global Dispersal of Aerosols	10
1.3.1. Asia.....	10
1.3.2. Europe.....	14
1.3.3. North America.....	15
1.4. Importance of Studying Atmospheric Aerosol Pollution	16
1.4.1. Public Health	16
1.4.2. Economy	17
1.4.3. Radiation and Climate.....	18
1.5. Purpose of Study	19
1.5.1. Why Sentinel?	19
1.5.2. Aims and Objectives.....	20
1.6. Outline of the Thesis.....	20
2. Literature Review	21
2.1. Aerosol Measurements	21
2.1.1. Particulate Matter.....	21
2.1.2. Aerosol Optical Depth.....	21
2.2. Current Research	25
2.2.1. Correlation	25
2.2.2. Current Limitations	27
2.3. Conclusions.....	27
3. Methodology.....	29
3.1. Study Regions	29
3.2. Satellite Datasets	29
3.2.1. Sentinel-3A AOD	29
3.3. Ground Datasets.....	31
3.3.1. PM _{2.5} Datasets.....	31
3.3.2. AERONET AOD.....	33

3.4. Methods	33
4. Results	34
4.1. Monthly Correlations.....	34
4.1.1. Correlation between PM _{2.5} and Sentinel-3a with comparisons to AERONET AOD.....	34
5. Discussion.....	43
6. Conclusions	44
Bibliography	45

Abstract

In this thesis, the linear correlation of remotely sensed aerosol optical depth (AOD) and ground-measured fine particulate matter ($PM_{2.5}$) is investigated. With instruments that are commonly used to derive the concentrations of $PM_{2.5}$ using remote sensing and AOD correlation, such as MODIS, going past its expected operation period, new instruments must be investigated to determine if they will be suitable for AOD and $PM_{2.5}$ studies in the future.

In this study, Sentinel-3a AOD data, derived from the Swansea University aerosol retrieval algorithm, was used to investigate the linear relationship between remotely sensed AOD and ground-measured $PM_{2.5}$ at the city scale. City pixels of AOD were correlated against aggregated $PM_{2.5}$ stations, and compared against the correlations of AERONET, a well-established ground measured AOD dataset, to see how they performed. This was conducted at a city-wide scale.

This study showed a similar performance in the R^2 values between Sentinel-3a and AERONET when correlating monthly values, but with R^2 values remaining low. The main conclusions were that Sentinel-3a datasets have the potential to estimate $PM_{2.5}$, but further research must be conducted in order to determine the best approach, as the city-scale may not be appropriate due to the coarse resolution.

1. Introduction

1.1. Motivation

Atmospheric aerosols can be defined as small, suspended particles, both solid and liquid, within the atmosphere. The size of aerosols can range from a few nanometers (nm) to hundreds of micrometers (μm), as they need to be small enough to be transported by winds and atmospheric turbulence (Wallace and Hobbs, 2006). Aerosols can be sourced both naturally and anthropogenically. On a global scale, natural sources are responsible for 90% of total aerosol concentrations, with sea salt being the largest contributor towards that figure as 71% of the Earth's surface is covered by the ocean (Pueschel, 1995; Visbeck, 2018). Dust particles, volcanic ash, pollen, and smoke are additional examples of natural aerosols. The release of these aerosols is independent from human activities, contrary to the anthropogenic sources that make up the remaining 10% of aerosol mass. In particular, population growth, industrialisation and economic growth have led to increased fossil fuel emissions. This has enhanced the production of fine, suspended particles, which have changed the chemical composition of our atmosphere. Accompanying the increase in atmospheric aerosols is the rapid decline in air quality associated with the burning of fossil fuels, vehicular emissions, and other anthropogenic activities. This is of increasing concern, as air quality can have significant effects on the environment, the economy, and public health.

UNICEF (2016) stressed the profound effects that air quality could have on the public, as 2 billion children worldwide live in regions where recognised international limits of air pollution have been breached, with 300 million of these existing in places where air pollution exceeds those targets by a factor of six. With the increased awareness of environmental changes in both the media and the public eye, especially those with anthropogenic origins, initiatives on the local and global scales are being pursued. One of the most notable is the United Nations Sustainable Development Goals (SDG), which came into effect on the 1st of January 2016, and are comprised of 17 SDGs and 169 targets that aim to curb environmental degradation and create a more equal society in all aspects. Air pollution and general air quality, whilst not a specific goal, features strongly in three SDGs; health (3), cities (11) and sustainable consumption and production (12). Additionally, Longhurst *et al.* (2018), citing both EEA (2017) and UNICEF (2016), noted that air quality impacts upon 12 of the 17 goals.

Henceforth, multiple international authorities have now recognised the importance in monitoring air quality and implementing measures to control and reduce pollutants, including understanding the composition and distribution of aerosol sources (McMurry *et al.*, 2004). However, there are still significant gaps in our knowledge of aerosol production, their movement, and their exact environmental effects. This makes it difficult to accurately measure atmospheric pollution in its entirety. Additionally, there are significant challenges in measuring aerosol concentrations. In-situ aerosol measurements tend to have poor spatial coverage and provide little insight to spatial variability, but they have a high degree of accuracy. On the other hand, using satellite derived aerosol measurements would provide larger datasets that cover a wider spatial area, but the accuracy may decrease with lower spatial resolution. Fortunately, there are widely accepted measurements of air quality that can be studied using both in-situ measurements and remote sensing instruments, namely particulate matter and aerosol optical depth, that can be used to predict aerosol concentrations.

1.2. Aerosol Measurements and Distribution

1.2.1. Particulate Matter

Whilst the definition of aerosols refers to both suspended matter and the suspending gas, the definition of particulate matter (PM), sometimes called particle pollution, refers to only the suspended particles that are considered in those aerosol measurements. PM can consist of both solid and liquid particles, as well as a variety of different materials; from metals to dust and sand, to chemicals such as nitrates or sulphates, and to carbonaceous materials. PM is usually sub-categorised into two classifications. All particles with an aerodynamic size of $10\mu\text{m}$ or lower are referred to as PM_{10} . This group contains coarse particles, which are often dust, pollen, ash and other naturally occurring substances that are transported atmospherically, as these tend to be between $2.5\mu\text{m}$ to $10\mu\text{m}$ in diameter. The other group is for fine particles only. Also referred to as $\text{PM}_{2.5}$, as they have an aerodynamic size less than $2.5\mu\text{m}$, these fine particles are often consisting of carbonaceous, inorganic materials, as mentioned above, that come from fossil fuel consumption. For comparison, a strand of human hair is $50\text{-}70\ \mu\text{m}$ in diameter.

Whilst, on a global scale, natural aerosols make up the majority of aerosol mass concentrations (Ramachandran *et al.*, 2012), hotspots of elevated aerosol levels are routinely found in dense, urban areas. These hotspots are associated with a noted increase in $\text{PM}_{2.5}$ levels in cities. This implies that the main sources of $\text{PM}_{2.5}$ are anthropogenic in origin rather than natural, as discussed previously (Ortiz *et al.*, 2017; Filonchik *et al.*, 2020). This ties in with how $\text{PM}_{2.5}$ concentrations have increased in recent years in line with urbanisation and globalisation. Danish *et al.* (2018) looked at how with globalisation the increase in ICT increased air pollution and found that a 1% increase in financial development stimulates emissions. However, there are multiple different sources of urban $\text{PM}_{2.5}$.

One such source is $\text{PM}_{2.5}$ from industrial factories, as PM pollution tends to originate from fossil fuel combustion (Phalen and Phalen., 2013). Vehicular emissions are another prominent source of $\text{PM}_{2.5}$. Lelieveld *et al.* (2015) found that land traffic emissions were responsible for approximately 5% of $\text{PM}_{2.5}$ related mortality globally, but this increases to 20% in countries such as Germany, the USA and the UK. This is because carbonaceous $\text{PM}_{2.5}$, which is emitted through the exhaust pipes of cars, is around five times more toxic than other types of $\text{PM}_{2.5}$. Ortiz *et al.* (2017) found that in Madrid the $\text{PM}_{2.5}$ exceedances that were slightly higher than those of PM_{10} due to the fact that diesel vehicle road traffic there is far greater. There are additional anthropogenic sources of $\text{PM}_{2.5}$ outside of cities. Lelieveld *et al.* (2015) found that agriculture is the leading source of $\text{PM}_{2.5}$ in Europe, Russia, Turkey, Korea, Japan and Eastern USA. This study found that agricultural $\text{PM}_{2.5}$ contributes $\geq 40\%$ of the total $\text{PM}_{2.5}$ levels in these regions, a figure which Giannakis *et al.* (2019) agreed with. However, most of the $\text{PM}_{2.5}$ consists of inorganic nitrates, as the agricultural $\text{PM}_{2.5}$ is often due to ammonia from fertilisers. Bauer, Tsigaridis and Miller (2016) found that significant reductions in $\text{PM}_{2.5}$ can be made by reducing either agricultural NH_3 or combustion NO_x , as agricultural pollution dominates over Europe, Central USA and Western China. Biomass burning is also a significant source of $\text{PM}_{2.5}$ in some countries. Lalitaporn and Mekaumnaychai (2020) found that Northern Thailand experiences air pollution haze episodes due to biomass burning, which lead to an increased number of hospitalisations, and Lelieveld *et al.* (2015) demonstrated that biomass burning contributes to 70% of $\text{PM}_{2.5}$ in Brazil, but only 5% globally.

It is $\text{PM}_{2.5}$ that is of particular concern to the general public due to the strong association with numerous adverse health effects. This is because these fine particles can embed themselves within human cells, most concerningly within the respiratory or cardiopulmonary system. Both short-term and long-term illnesses can be connected to this phenomenon, with symptoms such as inflammation, fever, and cardiac events, to much more permanent diseases such as asthma,

diabetes, and cancer (Loomis *et al.*, 2013; Lelieveld *et al.*, 2015). This leads to a larger mortality rate, demonstrated recently by the first death in the UK attributed directly to air quality by a coroner (Dyer, 2020). Whilst PM_{2.5} is considered harmful at low concentrations, with no lower value where PM_{2.5} is no longer a threat to human health, multiple governments and organisations have implemented national and regional standards for PM_{2.5} classification. The World Health Organisation (WHO) has an established PM_{2.5} limit of 25 µg m⁻³, and countries such as the US have limits of 35 µg m⁻³ for 24-hour maximum concentrations averaged out over three years (EPA, 2013). Additionally, PM_{2.5} has been found to be responsible for environmental degradation, affecting temperatures, radiation, climate, and visibility haze. Henceforth, PM_{2.5} concentrations will be the focus of this thesis.

1.2.2. Aerosol Optical Depth

Another commonly accepted measurement for aerosols is Aerosol Optical Depth (AOD). This is a dimensionless parameter related to atmospheric radiative transfer and is considered one of the most comprehensive variables to study aerosol load in the atmosphere using remote sensing (Wei *et al.*, 2020). Solar radiation interacts with atmospheric particles as it travels through the atmosphere, leading to radiative scattering and absorption. Scattering refers to when photons are dispersed in several directions after coming in contact with an atmospheric particle, such as aerosols or cloud particles. There are two main types of scattering; Rayleigh scattering, which is caused by atoms, molecules and other small particles, and Mie scattering, which occurs when there are large particles in the same size range as the radiation wavelength. Absorption, on the other hand, occurs when photons are converted into other energy forms (Mishchenko, Travis and Lacis, 2002). Both processes lead to the attenuation of solar radiation, or its reduction. The total amount of attenuation caused by these processes is referred to as the extinction. AOD measures the total amount of aerosols present in an atmospheric column by calculating the radiation extinction of a specific wavelength. The calculation for AOD is shown in Equation 1:

$$\tau_a(\lambda) = \int_0^x \sigma_{ext} dx$$

Equation 1: Equation to calculate Aerosol Optical Depth

Where τ_a is AOD, λ is the wavelength, σ_{ext} is the extinction coefficient, also defined as the depletion of radiation per unit length, and dx represents the unit cross section of a vertical atmospheric section.

Whilst PM_{2.5} only measures fine particulate of diameter 2.5µm or smaller, AOD is a measurement of all aerosols within an atmospheric column. Hence, AOD includes coarser particles that are omitted from PM_{2.5}, which often tends to be naturally occurring aerosols. Volcanic ash, smoke and pollen are all examples of aerosols that are included within AOD measurements, with coastal areas often having high values of AOD due to the presence of sea salt and other coarse particles such as water vapour. Filonchyk *et al.* (2020) found that high coastal AOD can also be the result of strong emissions from ships, as well as strong hygroscopic growth and long-range aerosol transport. Dust and sand also contribute to AOD totals, with places such as the Tarim Basin and the Gobi Desert in China have continually naturally elevated AOD levels, as the prevalence of desert dust is constant regardless of meteorological conditions. However, desert areas are often uninhabited, with dust and sand being the only sources of aerosols in these regions, so whilst AOD is naturally elevated the overall AOD total remains low. AOD is also affected by anthropogenic emissions. Filonchyk *et al.* (2020) identified that a high degree of urbanization, a high population density and high vehicular emissions lead to high aerosol loads. Xue *et al.* (2014) also made an important point that the distribution of the

aerosols that contribute to AOD is determined not only by the source but the transport of aerosols, with aerosol loading occurring in valleys due to mountains acting as a barrier to transmission.

AOD can also be attributed to a significant number of environmental effects, in the exact same manner as PM_{2.5}. The most noticeable of these is the effect on the radiation budget, as both the scattering and absorption of radiation by aerosols changes the rate at which atmospheric processes can occur, as they rely on the presence of light to either decompose or separate molecules from one another to cause new chemical reactions (Palancar *et al.*, 2013). This can cause a reduction in precipitation and the size of cloud droplets, which are both extremely important properties to consider in climate change modelling. These added uncertainties can drastically change the results of a climate predictive model and will limit our ability to be accurate with datasets that may influence policy decisions and future action.

1.3. Global Dispersal of Aerosols

1.3.1. Asia

Air quality in Asia has been discussed extensively in the literature, as the air pollution in the region is notably high. The literature discusses a multitude of reasons for the aerosol concentrations in Asia. Firstly, many Asian countries are emerging economies, currently undergoing urbanisation at a fast pace. China is the prime example here. Since China's reform on trade policy in the 1980's, trade volume has increased to 50% from 20% (Munir and Ameer, 2018). This has increased the rate of environmental degradation. This rapid financial growth and increasingly high trade rates is why studies such as Cohen *et al.* (2019) and Mi *et al.* (2015) reported China as being the largest greenhouse gas emitter, contributing 23% of global greenhouse gas emissions. 57% of China's emissions in 2007 were from fossil fuels (Feng *et al.*, 2013) with Filonchuk *et al.* (2020) finding that China consumed 641.2 million tonnes of oil, 243.3 million tonnes of oil equivalent of natural gas, and 1906.7 million tonnes of oil equivalent of coal, which is 13.8%, 7.4% and 50.5% of global consumption respectively.

The emission rates across Asia are not equal, however. Looking at the emission rates in other countries, the city of Lhasa in Tibet has experienced rapid urbanization, yet due to its isolated location and high renewable energy consumption, has low aerosol concentrations that are improving with effective air pollution control measures (Yin *et al.*, 2019). Bauer *et al.* (2016) reported that 80% of all PM_{2.5} in India is attributed to natural sources like desert dust, with around 20% being attributed to agriculture. Even in China, 57% of China's emissions are related to transporting goods and services to provinces outside of where they were created (Feng *et al.*, 2013). Liu *et al.* (2019) noted that Beijing-Tianjin-Hebei (BTH) is densely populated and highly polluted, yet the majority of the expected emissions to power such a populated region occur in different areas of China, as the affluent BTH region outsources more than 75% of its emissions in order to keep industrial factories separate from residential areas (Feng *et al.*, 2013). Sheel, Guleria and Ramachandran (2018) also highlighted the issue of aerosol loading at the foothills of the Indian Himalayas, meaning that aerosol concentrations in certain regions may be more affected by meteorological variables and topographical features than any one pollution source.

Air quality and emissions policies, particularly global ones enacted by organisations such as the IPCC and WHO, focus on Asia as a place that requires a large improvement in air quality, particularly as the economies develop and transition from industrial manufacturing to high-end goods and services (Cohen *et al.*, 2019). Multiple Asian countries have implemented policies to combat high pollution rates. Environmental regulations that have come into place in China since the 2008 Olympic Games, such as the commitment to reduce the carbon intensity of the economy by 40-45% at the 2009 Copenhagen Climate Change Conference, have since caused the AOD values in Beijing to decrease

(Xue *et al.*, 2014; Xue *et al.*, 2017; Feng *et al.*, 2013). Additionally, the Chinese government in September 2013 published the “Air Pollution Prevention and Control Action Plan”, which is a policy the Chinese government are implementing to decrease fine particulate matter concentrations by 15-25% depending on area (Huang *et al.*, 2018). Since then, total coal consumption has fallen by 300 million tons (Liu *et al.*, 2019), resulting in an overall decline in PM_{2.5} by 33.3% (Chen and Bloom, 2019), with reductions of 39.6% in BTH, 34.3% in the Yangtze River Delta, and 27.7% in Pearl River Delta (Liu *et al.*, 2019).

1.3.1.1. PM_{2.5}

In Asia, PM_{2.5} concentrations not only vary significantly between countries, but also between cities. A large portion of the literature has concentrated research in the highly polluted BTH region of China, which includes the city of Beijing, where PM_{2.5} are often significantly higher, usually by a factor of 5, than recommended levels (Kong *et al.*, 2016; Chen & Bloom, 2019). Table 1 presents a compilation of reported values of PM_{2.5} from studies conducted in Asia.

Table 1: Summary of PM_{2.5} studies conducted in Asia, with columns denoting the average/mean PM_{2.5} value found, the peak PM_{2.5} value found, the time period over which the study was conducted, and a notes column that provides information on how the values were calculated.

Region	Study	Values		Time Period	Notes
		Average/Mean	Peak		
Beijing, China	Huang <i>et al.</i> (2018)	57 µg m ⁻³	N/A	2017	Ground-measured station
	Kong <i>et al.</i> (2016)	62 ± 45 µg m ⁻³	N/A	2009 - 2010	Compared to a background level of 36 ± 29 µg m ⁻³ and a suburban level of 79 ± 61 µg m ⁻³
	Zhou <i>et al.</i> (2015)	85.81 µgm ⁻³	800 µg m ⁻³	2013	Ground-measured station
Shanghai, China	Kan & Chen (2004)	100 µg m ⁻³	N/A	2001	Compared to a background level of 73.2 µgm ⁻³
Northern China	Xin <i>et al.</i> (2014)	33 ± 10.2 µg m ⁻³	44.4 µg m ⁻³	2009 - 2011	Ground-measured station
Tibetan Plateau	Xin <i>et al.</i> (2016)	10 - 117 µg m ⁻³	N/A	2011 - 2014	Ground-measured station
Lhasa, Tibet	Yin <i>et al.</i> (2019)	22.74 ± 23.92 µg m ⁻³	N/A	2013 - 2017	Ground-measured station
Northern Thailand	Lalitaporn & Mekaumnuaychai (2020)	N/A	357 µg m ⁻³	2014 - 2017	
Delhi, India	Kumar, Chu and Foster (2007)	82.9 ± 7.8 µg m ⁻³	N/A	August-November 2003	
Kolkata	Jain and Sharma (2020)	58 µg m ⁻³	N/A	March-April 2019	Ground-measured station

Bangalore	Jain and Sharma (2020)	35 $\mu\text{g m}^{-3}$	N/A	March-April 2019	Ground-measured station
Mumbai	Jain and Sharma (2020)	37 $\mu\text{g m}^{-3}$	N/A	March-April 2019	Ground-measured station
Seoul, South Korea	Kim <i>et al.</i> (2019)	45.7 $\mu\text{g m}^{-3}$	N/A	2014	MODIS AOD derived

As shown from the table, studies routinely find that PM_{2.5} in Asia is above the WHO recommended levels of 25 $\mu\text{g m}^{-3}$. Xin *et al.* (2014) studied PM_{2.5} concentrations from 2009 to 2011 in North China was $33 \pm \mu\text{g m}^{-3}$, with a maximum value hit in the summer of 44.4 $\mu\text{g m}^{-3}$ with a minimum in the winter of 25.3 $\mu\text{g m}^{-3}$. This was at least three times higher than what was being observed in Europe and the USA during that time period. Meanwhile Lalitaporn & Mekaumnaychai (2020) reported that average daily PM_{2.5} levels of 357 $\mu\text{g m}^{-3}$ in Northern Thailand for the 2014-2017 period, which is a factor of 14 times higher than the WHO guidelines of 25 $\mu\text{g m}^{-3}$, with higher PM_{2.5} values found in the morning than in the afternoon, and also in the pre-monsoon season of March-April. All stations in the study Xin *et al.* (2016) conducted in the Tibetan Plateau exceeded the WHO guidelines as well, with the study finding a maximum value of 1415 $\mu\text{g m}^{-3}$ occurring during a dust storm and a minimum value of 0.6 $\mu\text{g m}^{-3}$ occurring during the clearest day.

There are significant spatio-temporal variations in PM_{2.5} concentrations throughout Asia. Xin *et al.* (2016) found significant spatial variation between North and South China as well, at 57.3 $\mu\text{g m}^{-3}$ and 46.4 $\mu\text{g m}^{-3}$ respectively. This is likely due to the abundance of urban agglomerations in North China and a high number of industrial aerosols. Kong *et al.* (2016), looking at a city scale, attributed higher PM_{2.5} values to industrialisation, as the suburban region of Beijing had a higher value of $79 \pm 61 \mu\text{g m}^{-3}$ compared to the city centre value of $62 \pm 45 \mu\text{g m}^{-3}$, likely due to the relocation of manufacturing factories. 30% of daily mean values are above 75 $\mu\text{g m}^{-3}$ in this suburban region. Yin *et al.* (2019) found that in Lhasa, Tibet, there was a December maximum value of $40.88 \pm 42.88 \mu\text{g m}^{-3}$ and a July minimum value of $14.58 \pm 13.48 \mu\text{g m}^{-3}$, with peaks occurring in the morning and evening.

Since air pollution measures have been enacted in the region however, PM_{2.5} concentrations have been 20.6% to 43.1% lower (Wang *et al.*, 2019), with Huang *et al.* (2018) corroborating that study with its study that found PM_{2.5} concentrations have decreased 33.3%, from 72.2 $\mu\text{g m}^{-3}$ to 47.0 $\mu\text{g m}^{-3}$ between 2013 and 2017 in 74 cities. P. Wang *et al.* (2020) found that by modelling a reduced emissions pathway, PM_{2.5} concentrations decreased by up to 20% compared to no change, with an absolute decrease of 9.23 $\mu\text{g m}^{-3}$ in Beijing, and 30.79 $\mu\text{g m}^{-3}$ in Wuhan.

1.3.1.2. AOD

Similar to PM_{2.5}, AOD measurements in particular regions of Asia are also high. Peak AOD values in Asia are often associated with urbanization. Filonchik *et al.* (2020) found that the three main components of the AOD, which account for about 60% of the value, were found to be sulphates, black carbon, and organic carbon, with peak values in the BTH region of China being associated with coal-fired power stations. Dust is also a large contributor to AOD measurements in Asia, with high AOD values of 0.8 in the Gobi Desert due to natural dust emissions (Acharya *et al.*, 2021). Table 2 presents a selection of studies that have looked at AOD in Asia.

Table 2: Summary of AOD studies conducted in Asia, with columns denoting the average/mean AOD value found, the peak AOD value found, the time period over which the study was conducted, and a notes column that provides information on how the values were calculated.

Region	Study	Values		Time Period	Notes
		Average/Mean	Peak		

South East Asia (Thailand, Laos, Vietnam, Bangladesh and Eastern China)	Acharya <i>et al.</i> (2021)	0.6 - 0.8	N/A	2017 - 2019	Combination of MODIS derived AOD and AERONET AOD
Beijing, China	Kong <i>et al.</i> (2016)	0.53 ± 0.47	N/A	2009-2010	MODIS derived AOD Compared to a background level of 0.24 ± 0.22 and a suburban level of 0.54 ± 0.46
Northern China	Xue <i>et al.</i> (2017)	N/A	0.8	1983-2015	AVHRR derived AOD, cross- validated with AERONET AOD
	Xin <i>et al.</i> (2014)	0.23 ± 0.10	0.33	2009 - 2011	Combination of ground measured AOD using a portable sun photometer and MODIS AOD
	Filonchuk <i>et al.</i> (2020)	N/A	0.8	2019 - 2020	MODIS derived AOD
Western China	Acharya <i>et al.</i> (2021)	0.4 – 0.6	N/A	January – April 2020	Combination of MODIS derived AOD and AERONET AOD
	Filonchuk <i>et al.</i> (2019)	N/A	0.8 ± 0.1	2000 – 2017	Combination of MODIS derived AOD and MISR derived AOD
Eastern China	Filonchuk <i>et al.</i> (2019)	0.521 – 0.828	N/A		
Tibetan Plateau	Filonchuk <i>et al.</i> (2019)	0.025 – 0.223	N/A	2000 – 2017	Combination of MODIS derived AOD and AERONET AOD
Delhi, India	Kumar <i>et al.</i> (2007)	0.65 ± 0.025	N/A	October - November 2003	MODIS derived AOD

AOD values in Asia demonstrate that the air quality is often polluted. Xin *et al.* (2014) found that AOD in Asia was 2 times higher than background levels. In the same manner as PM_{2.5}, there are spatio-temporal variations in the measurements of AOD in Asia. In terms of seasonal variations, dust was a factor that mainly affected spring time AOD, demonstrating that there are strong seasonal variations that lead to AOD maxima in the summer and minima in the winter, with an AOD peak of 1.2 in the summer. Similar values were reported in Xin *et al.* (2014), which identified the annual mean AOD of Northern China between 2009 to 2011 to be 0.23 ± 10 , with a summer maximum value of 0.33 and a winter minimum of 0.14. Spatially, there are lots of variations. Notably, whilst AOD can vary significantly temporally in one region, in other regions there will be a lot less variance. In Asia, this tends to be in desert regions such as the Gobi Desert, where AOD measurements are naturally elevated but remain low compared to urban agglomerations.

1.3.2. Europe

Compared to Asia, the amount of recent literature on Europe’s air quality is small. This could be attributed to Europe’s developed economies and associated air quality problem being well established. Coupled with an ageing populations and ever-increasing urbanisation there is still cause for concern, even if the situation is not as serious as with Asia. In terms of spatial distribution, Northern Italy is one of the most polluted areas, particularly in Lombardia and Emilia Romagna, due to high emissions and geographic conditions that caused the stagnation of pollutants (Conticini, Frediani and Caro, 2020). Bauer *et al.* (2016) found that agricultural PM_{2.5} is responsible for 55% of air pollution.

There has been some improvement in recent years, particularly with the implementation of air pollution policies. In the UK, the Clean Air Act was passed in 1956 to address the issue of smoke pollution (Huang *et al.*, 2018), and a new Air Quality Directive established in 2008 set an annual mean PM_{2.5} target of 25 µg m⁻³. Additionally, there was the collective aim to reduce road emissions by 83%, machinery emissions by 54% and energy production by 32% (Schneider *et al.*, 2020). Giannakis *et al.* (2019) noted that PM_{2.5} emissions have fallen by 28% between 2008 to 2015. Other studies have noted, however, that the drop in emissions may be due to other factors aside from air quality measures. Sanchez de la Campa (2014) found that during the 2008 financial crisis there were decreases in PM, with chemical components becoming more pronounced, in the South of Spain. This is due to the loss of industrial production associated with factory foreclosures.

1.3.2.1. PM_{2.5}

PM_{2.5} in Europe varies spatially, as some regions have relatively low values whilst others have significantly high pollution levels. In terms of PM_{2.5} values found across the continent, the WHO threshold of a 24-hour average of 25 µg m⁻³ was found to be exceeded at 66% of monitoring stations across the 27 member states of the European Union (EU) and the UK (Ortiz *et al.*, 2017). Table 3 collects PM_{2.5} values from studies conducted in Europe.

Table 3: Summary of PM_{2.5} studies conducted in Europe, with columns denoting the average/mean PM_{2.5} value found, the peak PM_{2.5} value found, the time period over which the study was conducted, and a notes column that provides information on how the values were calculated.

Region	Study	Values		Time Period	Notes
		Average/Mean	Peak		
United Kingdom	Schneider <i>et al.</i> (2020)	9.41 µg m ⁻³	N/A	2008	Derived from MODIS AOD using machine learning
		10.17 µgm ⁻³	N/A	2013	
		8.05 µgm ⁻³	N/A	2018	
Italy	Giannakis <i>et al.</i> (2019)	6 - 8 µg m ⁻³	N/A		Derived from an atmospheric chemistry model
	Buonanno <i>et al.</i> (2015)	40.8 µg m ⁻³	N/A	2017 - 2021	
Balkan Countries (Bulgaria, Romania, Slovenia)	Giannakis <i>et al.</i> (2019)	9 - 10 µg m ⁻³	N/A		Derived from an atmospheric chemistry model

Countries such as those located in the Balkan region of Europe are considered polluted, with Giannakis *et al.* (2019) finding that the highest PM_{2.5} values occurred in these regions, with the lowest in Slovakia and Spain. Schneider *et al.* (2020) found significant spatial variations from the period average of 8.84 µg/m³, with PM_{2.5} hotspots found in dense English cities such as Birmingham, Liverpool, London, and Manchester, with lows in the Scottish and Welsh countryside. Studying the

values of PM_{2.5}, alongside PM₁₀, across Spain, Ortiz *et al.* (2017) also found significant spatial variations as well. Relating these values to the WHO threshold, Madrid monitoring stations reported exceedances 14.9% of days in the 2000-2009 period, with Gran Canaria and Tenerife exceeding the threshold 7.9% and 7.2% of days respectively. Temporal variations were also frequent, with meteorological conditions causing patterns such as a north-south split, or with pollution hotspots over dense cities, to days where there is general uniformity across the country. De la Campa & de la Rosa (2014) found hourly maximums at early morning as well as late night, which was pronounced during the summer. This study attributed this temporal variation to ceramic industry activity and road traffic.

1.3.2.2. AOD

AOD measurements in AOD demonstrate a similar pattern to PM_{2.5}. AOD levels in Europe tend to be a lot lower than in Asia, with higher values reserved for heavily industrialised areas (Xue *et al.*, 2017). Table 4 shows a selection of AOD studies in Europe.

Table 4: Summary of AOD studies conducted in Europe, with columns denoting the average/mean AOD value found, the peak AOD value found, the time period over which the study was conducted, and a notes column that provides information on how the values were calculated.

Region	Study	Values		Time Period	Notes
		Average/Mean	Peak		
Europe	Xue <i>et al.</i> (2017)	>0.5			AVHRR derived AOD, cross-validated with AERONET AOD
Poland	Zielinski <i>et al.</i> (2016)	0.114	0.413	1999 - 2003	AERONET AOD
Sweden	Zielinski <i>et al.</i> (2016)	0.089	0.317	1999 - 2003	AERONET AOD
Belarus	Zielinski <i>et al.</i> (2016)	0.224	0.557	1999 - 2003	AERONET AOD
Switzerland	Nyeki <i>et al.</i> (2012)	0.025 – 0.068	0.23	1995 - 2010	
Germany	Nyeki <i>et al.</i> (2012)	0.104		1995 - 2010	

AOD levels in Europe remain fairly low. Spatially, Xue *et al.* (2017) did find variations, with low values being reported in the mountainous regions of the Alps, and high values of 0.3 being found in the industrialised areas of Hungary, Croatia, and the Po Valley in Italy. Acharya *et al.* (2021) used both MODIS and AERONET to find mean AOD values of 0.2-0.3 in Eastern Europe, and values of <0.2 in the West, with Meier *et al.* (2012) concurring. Temporally however, Xue *et al.* (2017) did not find significant annual changes, with AOD remaining under 0.2 for the majority of the continent. However, there were seasonal variations between the spring and summer months and winter. AOD levels have also been seen to vary temporally when there is a large environmental event in Europe, such as a wildfire. Zielinski *et al.* (2016) found that AOD levels peaked in Eastern Europe during the August 2002 wildfires, with fine particles being dominant and that meteorological variables such as slow wind speeds exacerbating these conditions. Meanwhile Nyeki *et al.* (2012) found a peak value of 0.23 after the 1991 Pinatubo eruption. A noteworthy observation was that altitudinal differences had an effect on AOD as it changed how the planetary boundary layer and other meteorological conditions impact AOD. This observation was found to be statistically significant at the 95% confidence level at three different sites, likely due to changes in relative humidity and atmospheric circulation (Bian *et al.*, 2009; Chiacchio *et al.*, 2011). Mishchenko and Geogdzhayev (2007) found a significant decrease of ~0.024 per decade over most of Europe, which de Meij *et al.* (2012) agreed with.

1.3.3. North America

Air pollution levels in North America are comparable to ones found in Europe. Wang *et al.* (2003) noted that unhealthy pollution levels have occurred in the US, as stagnant air resulting from a

northern high-pressure system and a southern low-pressure system accumulated in the Ohio and Mississippi river valleys provided the best conditions for haze accumulation. Bauer *et al.* (2016) found that anthropogenic sources contribute 60% of PM_{2.5}. This study also found that the Eastern US has annual mean concentrations above 14 µg m⁻³ with agriculture being responsible for about half of this value. Food production produces the same amount as all other human activities combined such as motor vehicles, and approximately half of PM_{2.5} in eastern US is inorganic and primarily ammonium, nitrate, and sulphate.

The US has also put in place air pollution control measures. Huang *et al.* (2018) noted that since the Clean Air Act was passed in 1970 and amended in 1977 and 1990, concentrations of PM_{2.5} have reduced by 37% from 1990 compared to 2015. Total emission rates have decreased by 78% since 1970 (US EPA, 2021).

1.3.3.1. PM_{2.5}

Wang *et al.* (2003) looked at air pollution in the US. This study found that the majority of PM_{2.5} values were around 20 µg m⁻³, with around 20% of the PM_{2.5} values being greater than 40 µg m⁻³. This study also found diurnal changes in the concentration of PM_{2.5}, with a sharp increase from 6-8 AM each day, which then declines until it begins to rise after 2 PM. This appears to be due to traffic flow patterns and changes in the boundary layer, as solar heating causes PM_{2.5} concentrations to rise. Liu *et al.* (2004) found the range of PM_{2.5} to be from 4.72 to 20.51 µg m⁻³ with the mean being 10.76 µg m⁻³. That is three times less than North China.

Van donkelaar (2006) found that there was a seasonal maximum in the northern US. Quintana *et al.* (2015) looked at PM_{2.5} in California and found that there were higher PM concentrations in the winter than in the summer. The topography of the region affected PM_{2.5} concentration by having a low atmospheric mixing height. Meanwhile, south-eastern concentrations are largely driven by fires.

1.3.3.2. AOD

There is not as much literature on American AOD when compared to the vast amount of studies on AOD in Asia and Europe, which shows a significant gap in AOD knowledge that requires more research. Wang *et al.* (2003), using MODIS AOD, found AOD values of 0.35 in July to September and 0.1 in the winter months. Achayra *et al.* (2021) found that AOD in the Eastern US was around 0.1-0.2.

1.4. Importance of Studying Atmospheric Aerosol Pollution

1.4.1. Public Health

PM_{2.5} is related to both morbidity, which is when a population suffers from a disease but does not die from it, and mortality, where a population does die from a disease (Kan and Chen, 2004). PM_{2.5} can embed itself both in the respiratory system and pulmonary alveoli and cause inflammation. This leads to oxidative stress and, in some cases, causes the release of antigens that are responsible for immunodepression (Ortiz *et al.*, 2017; Peters *et al.*, 2001). Hence, there would be a rise in the incidence of non-communicable diseases (NCD's), which are diseases that cannot be spread from person to person. Svendsen *et al.* (2007) demonstrated this in a paediatric study, showing that muted responses from immunoinflammatory biomarkers alongside an increase in PM_{2.5} led to reduced pulmonary function, leading to large increases in bronchitis, pneumonia, severe asthma, some allergies, and cardiovascular diseases such as chronic obstructive pulmonary disease (COPD) (Dutheil *et al.*, 2020; Giannakis *et al.*, 2019; Ortiz *et al.*, 2017). PM_{2.5} has also been classified as a carcinogen, and exposure to high levels can result in multiple forms of cancer (Loomis *et al.*, 2013; Burnett *et al.*, 2014). Additionally, PM_{2.5} has been found to be responsible, in some cases, for kidney disease, diabetes, and abnormal neurological development of children (Brook *et al.*, 2008; Freire *et al.*, 2010). Exposure to PM_{2.5} may also exacerbate already existing mortality issues. Contincini *et al.*

(2020) found that lethality from COVID-19 was much higher in the polluted regions of Italy (12%) compared to the average (4%). Tarin-carrasco *et al.* (2019) found that short and long-term exposure to PM_{2.5} can be reversible in as short a period as a year, as the human body can heal partially once exposure ends.

The Global Burden of Disease study estimates that there were 3.2 million premature deaths in 2010 that could be attributed to PM_{2.5}, or 5% of all global premature deaths (Lee *et al.*, 2015; Lelieveld *et al.*, 2015; Giannakis *et al.*, 2019). In contrast, Dutheil, Baker and Navel (2020) estimated that 4.6 million people die each year from air quality related diseases, which is lower than the value the World Health Organisation gave in 2014 that 7 million people died prematurely in 2012. Chen and Bloom (2019) found that air pollution was linked to 18.1% of deaths related to NCD's in 1990 and 13.1% in 2015. China has the highest rate of PM_{2.5} related deaths per year at 1.36 million, or 4000 deaths per day, which is an order of magnitude higher than the deaths from HIV/AIDS or road traffic accidents (Lelieveld *et al.*, 2015; WHO, 2014). In the US there are around 160,000 PM_{2.5} related premature deaths, whilst in Europe studies estimates there are around 400,000 premature deaths per year (Im *et al.*, 2018; Tarín-Carrasco *et al.*, 2019; Giannakis *et al.*, 2019; Lelieveld *et al.*, 2015). Hence, exposure to ambient particulate matter pollution has been named one of the top 10 leading global risk factors for disease. Current research suggests that reducing PM_{2.5} emissions will have a significant impact on mortality (Lee *et al.*, 2015; Tarin-carrasco *et al.*, 2019), with Im *et al.* (2018) finding that 54,000 and 27,500 premature deaths in Europe and the USA respectively could be avoided if global anthropogenic emissions decreased by 20%.

The literature differs on the number of deaths that can be attributed to air pollution as well as general mortality rates. Tarin-Carrasco *et al.* (2019) identified that this may be due to issues quantifying the number as spatio-temporal variations, differences in lifestyle habits, and the composition and relative toxicity of pollutants all differ throughout the models used in studies. Additionally, multiple studies consider the WHO threshold of 25 µgm⁻³ for their morbidity and mortality rates, where the PM_{2.5} values below this threshold are assumed 'safe' and are often discarded. Ortiz *et al.* (2017) stated that this may be a fallacy, where there is no safety threshold as PM_{2.5} exposure has a linear effect on mortality and up to 90% of mortality occurs below this concentration. Additionally, Giannakis *et al.* (2019) made clear that determining a mortality rate estimate needs to consider factors outside of just a general population, including population density and the non-linearity of exposure functions that occur when regions have low reference pollution rates compared to regions with elevated background levels, for example Scandinavian countries have a larger increase in mortality from a small rise in pollution levels, especially when compared to an area like Greece. Im *et al.* (2018) noted that studies that look at public health have not studied individual particle species such as purely carbonaceous PM, differences such as age, gender, ethnicity, and behaviour were not considered, and that exposure response functions often only consider urban background levels. There is also a lack of studies in certain regions, with Lim *et al.* (2022) finding that of 140 health related PM_{2.5} exposure studies, 49 were conducted in Asia, 45 in North America and 29 in Europe, with a noticeable research gap in North Africa, West Asia and Oceania.

1.4.2. Economy

Coupled with the effects on public health, poor air quality can have a devastating impact on the economy. Chen and Bloom (2019) detailed this process: an unhealthy population equals low productivity, particularly affecting school attendance and labour supply. This is referred to as the morbidity effect, where people suffer from a disease which does not kill them and their contribution to economic output decreases, such as decreasing the amount of time they can work in a day, being less educated due to not being able to attend school regularly and having to retire at an earlier age

due to poor health (Liu *et al.*, 2019). In addition, there is also the mortality effect, when working age individuals die from a disease and there is economic loss from the loss of human capital, and the treatment cost effect, when households need to use a significant portion of their savings to cover out-of-pocket treatment costs. Accompanied by governments needing to increase investments into NCD treatments to deal with a rising chronically ill population, poor air quality can lead to massive economic fallout.

There are multiple methods to calculate the economic losses associated with air pollution, but one of the most common is to attribute a financial value for a single person. This figure, known as the value of a statistical life (VOSL), is based on the amount of money a society is willing to pay (WTP) in order to prevent a premature death (Carvour *et al.*, 2018). The VOSL is often estimated by observing the risks people are willing to undertake and how much they should be paid for performing them, considering factors such as wages, the dangers present in a job, future earnings, life expectancy etc. Carvour *et al.* (2018), for example, assigned a value of approximately \$8 million to each air pollution attributable death in Texas, USA. VOSL is study region specific, as it is dependent on an individual's wage and is affected by income inequalities, and often appears as a probability where a maximum value of 1 represents certain death of an individual (Kim *et al.*, 2019).

In China, the total economic losses due to NCD's is estimated to be \$1137 billion from 1990-2030, with air pollution accounting for 0.72-10% of regional GDP loss depending on the study site, with cities such as Shanghai seeing a loss of 1.03% of GDP, or US\$624.4 million (Chen and Bloom, 2019; Kan and Chen, 2004). The economic impacts of air quality were EUR300 billion and EUR145 billion per annum in Europe and the USA respectively and is expected to increase by 17% by 2100 (Im *et al.*, 2018; Tarin-Carrasco *et al.*, 2019). Im *et al.* (2018) additionally quoted the OECD (2014) study that found that air pollution costed the member states a total of \$1.57 trillion in 2010, and that 89% of air pollution costs are attributed to PM_{2.5}. There are also specific regional studies. Tian and Chen (2007) found that Ontario was burdened by CAN\$9.6 billion in health damages per year. Kim *et al.* (2019) found that South Korea was predicted, out of all the OECD members, to suffer the worst economic damage. For these values, Kan and Chen (2004) found that premature deaths accounted for 82.9% of the total costs, with the cost of chronic respiratory diseases being the second biggest contributor.

1.4.3. Radiation and Climate

Aside from the impacts that aerosols can have on society, there are significant environmental effects as well. As mentioned previously, aerosols play a significant role in the Earth's energy budget and can scatter and absorb shortwave and longwave radiation from the sun, and a change in aerosol concentration can cause both direct and indirect radiative forcing. This can offset warming in some cases (Xue *et al.*, 2017) or exacerbate it in others (Zielinski *et al.*, 2016). For example, by reflecting solar radiation, aerosols cause less solar radiation to hit the surface, which would cool the surface. Conversely, if the radiation is absorbed, then a warming effect on the surface will be observed. Radiative forcing can also reduce solar irradiance, prevent aerosols from being removed from the atmosphere or disperse pollutants further, and cause changes to meteorological effects such as temperature or rainfall patterns (Sahu *et al.*, 2020; Rosenfeld *et al.*, 2002).

Zhang, Wen and Jang (2010) found that there was a reduction of solar radiation by -9.1%, or 11.3Wm⁻², in January 2001 purely due to the aerosol-radiation interactions. These numbers increase to -16.1% and 39.5Wm⁻² for July 2001. Associated with these reductions is the decrease of near-surface temperatures, ranging from 0.16 °C to 0.40 °C, and the reduction of the planetary boundary height layer by up to 24%, or 40-200m (Yang *et al.*, 2020a). The IPCC (2013) report found that there was a negative effect on direct radiative forcing between -0.9 and 0.1Wm⁻², with an indirect cloud

albedo forcing between -1.8 and -0.5Wm^{-2} . Aerosols also have a direct impact on UV radiation (Torres *et al.*, 2007; Graber and Rudich, 2006)

Our knowledge of radiative forcing due to aerosols is limited, however. It is difficult to quantify the mixing of aerosols in the planetary boundary layer, as well as the impact meteorological conditions have. These factors are equally as difficult to model (Petelski *et al.*, 2014), and this uncertainty is a large part of why global climate change estimates continue to have large variations (Dubovik *et al.*, 2019).

1.5. Purpose of Study

The previous sections have established the importance of measuring the concentrations of aerosols, namely $\text{PM}_{2.5}$, and how they vary spatially and temporally. This is in order to study the societal and environmental impacts of aerosols. Additionally, examples of aerosol studies were presented to show current ranges of PM and AOD in certain regions. The tables presented in these sections note the method that was used in order to measure the aerosol concentrations in each study, which will be explored further in future chapters. There are a multitude of different methods that can be used to derive aerosol concentrations, each with their benefits and limitations. $\text{PM}_{2.5}$ can be measured in-situ in ground measuring stations, whilst AOD is usually algorithmically derived from remote sensing instruments, such as ones found on satellites. Due to this, a lot of $\text{PM}_{2.5}$ datasets have limited spatial resolution due to the instruments on the ground only being able to measure the ambient aerosol concentration in the immediate proximity of the ground station.

To improve the spatial resolution of $\text{PM}_{2.5}$ datasets, multiple studies have identified the correlation between $\text{PM}_{2.5}$ and AOD (Wang & Christopher, 2003; Strandgren *et al.*, 2014; Shi *et al.*, 2018; Ma *et al.*, 2014). The temporal continuity and spatial coverage of remotely sensed AOD datasets makes its retrieval particularly valuable for $\text{PM}_{2.5}$ estimation, as strong correlations have been identified. AOD is an effective proxy for $\text{PM}_{2.5}$ when the particles are distributed evenly in the lower atmosphere (van Donkelaar, Martin and Park, 2006). One of the big limitations is that a lot of the current research tends to use the same instruments, especially AOD studies. This can be seen clearly in the tables presented earlier in the chapter, where a large majority of AOD studies have derived measurements from the Moderate Resolution Imaging Spectroradiometer (MODIS), which is onboard NASA's polar-orbiting satellite TERRA. MODIS datasets have frequently been applied to improve estimates of $\text{PM}_{2.5}$, especially when $\text{PM}_{2.5}$ ground monitors are not available. MODIS has had a mixed degree of success in estimating $\text{PM}_{2.5}$, with 10km, 3km and 1km spatial resolution products available. However, MODIS has a limited lifespan and has outgrown its expected operation period (Yao *et al.*, 2018, Schneider *et al.*, 2019). Henceforth, we will need to consider using new instruments in order to continue vital air quality research. This thesis will look into the possibility of the SLSTR instrument onboard Sentinel-3 as an alternative to MODIS.

1.5.1. Why Sentinel?

The aim of this thesis is to continue research into the linear relationship between ground measured $\text{PM}_{2.5}$ datasets and satellite derived AOD. Whilst well researched there is still a lot of uncertainty in modelling $\text{PM}_{2.5}$ from AOD, namely from how aerosols are retrieved from remotely sensed datasets and how AOD is calculated algorithmically. Additionally, there may be constraints with the orbit, design, and geometry calculations of the instrument. Henceforth, the suitability of a particular instrument for AOD and $\text{PM}_{2.5}$ studies must be carefully observed.

The European Commission's Copernicus Programme, which is an Earth Observation scheme, has launched the Sentinel-3 mission. This mission has been designed for the long-term collection of high-quality ocean, land and atmospheric measurements. One of the main objectives of the mission is to

measure atmospheric conditions over the sea and land with a high degree of accuracy and reliability (Berger *et al.*, 2012), in order to continue the datasets of the Environmental Satellites (ENVISAT) Advanced Along-Track Scanning Radiometers (AATSR) which have been discontinued. Sentinel-3 comprises of two satellites. Sentinel-3A was launched on the 16th of February 2016 and Sentinel-3B was launched on the 25th of April 2018. The two satellites operate simultaneously in orbit, but with 180° dephasing. The instrument that captures AOD is the Sea and Land Temperature Radiometer (SLSTR).

Even though it has been running since 2017, there is little to no literature using Sentinel 3a AOD. Henceforth, this thesis will be examining whether the SLSTR instrument onboard Sentinel-3a is suitable for linear regression studies, or even as a replacement for MODIS. In order to do so, we will be comparing linear regression graphs against an instrument that has been well established in air quality research, AERONET, which is a ground monitored AOD dataset.

1.5.2. Aims and Objectives

The aim of this thesis is to determine if Sentinel-3a AOD could be used to estimate PM_{2.5}.

The objectives are to:

1. Create monthly aggregated PM_{2.5} datasets, Sentinel-3a AOD datasets and AERONET AOD datasets.
2. Create linear regressions graphs of Sentinel-3a vs. PM_{2.5} and AERONET AOD vs. PM_{2.5}. Linear regressions will be created for the 550nm, as this is the standard wavelength that the majority of AOD studies use, 870nm, to see how the correlation differs between the two wavelengths, and fine mode AOD wavelengths, so that it can be observed if there is a significant difference between the correlations when only finer particles are included in the AOD.
3. Compare the R^2 , slopes and intercepts to determine the relative performance of AERONET and Sentinel-3a.

1.6. Outline of the Thesis

In chapter 1 the topic of this thesis has been introduced. The concepts of PM_{2.5} and AOD were defined, as well as showing where current research interests lie. The purpose and goal of this study, particularly why Sentinel-3a datasets should be studied, were explained alongside the aims and objectives.

In chapter 2 an in-depth literature review is presented to provide context to this study, particularly looking at current spatial PM_{2.5} and AOD characteristics, and more comprehensive information about the effects poor air quality can have.

Chapter 3 will describe both the methodology and the datasets used in this thesis. Information will be given about the data processing, where the data was collected from, which regions were investigated and what time periods will be studied.

Chapter 4 and 5 will present the results of this study and discuss the findings, and chapter 6 will sum up and talk about future studies.

2. Literature Review

2.1. Aerosol Measurements

2.1.1. Particulate Matter

Whilst PM_{2.5} is considered harmful at low concentrations, with no lower value where PM_{2.5} is no longer a threat to human health, multiple governments and organisations have implemented national and regional standards for PM_{2.5} classification. The World Health Organisation (WHO) has an established PM_{2.5} limit of 25 µgm⁻³, and countries such as the US have limits of 35 µgm⁻³ for 24-hour maximum concentrations averaged out over three years (EPA, 2013). Table 5 shows the defined air quality levels for the US and the UK, as two examples of how different countries monitor and communicate air quality (EPA, 2012).

Table 5: Left table demonstrates the Air Quality Level classifications for the US, and the right table presents the air quality index classifications for the UK.

Daily Mean Concentration (µgm ⁻³)	Air Quality Level (US)	Daily Mean Concentration (µgm ⁻³)	Air Quality Index (UK)
0.0 – 12.0	Good	0 – 11	1 (Low)
12.1 – 35.4	Moderate	12 – 23	2 (Low)
35.5 – 55.4	Unhealthy for Sensitive Groups	24 – 35	3 (Low)
55.5 – 150.4	Unhealthy	36 – 41	4 (Moderate)
150.5 – 250.4	Very Unhealthy	42 – 47	5 (Moderate)
250.5 - 500	Hazardous	48 – 53	6 (Moderate)
		54 – 58	7 (High)
		59 – 64	8 (High)
		65 – 70	9 (High)
		71 +	10 (Very High)

Conventionally, ground monitoring networks are used to sample and measure the amount of PM_{2.5} present in the atmosphere. This often limits the measurements that can be taken, as not only does the number and density of stations vary from city to city, and then country to country, but PM_{2.5} values can vary massively even between nearby stations. Additionally, there has been an historical lack of spatio-temporal coverage of PM_{2.5} worldwide. Schneider *et al.* (2020) noted that ground-monitored network stations in the UK are only concentrated in dense, urban areas, and it was only from 2010 onwards that wider measurements became available. Worldwide monitoring using these ground-based stations are difficult considering these factors, as one station may not be indicative of the average in the area.

2.1.2. Aerosol Optical Depth

A high AOD value means there are high aerosol concentrations. Table 6, with credit from Levy *et al.* (2013) demonstrates the relative expected conditions for a range of AOD values.

Table 6: AOD classification for Air Quality

AOD	Air Quality Condition
0	Clear
0.02	Very clean
0.2	Fairly clean
0.6	Polluted
1.5	Heavy smoke/dust

AOD can be measured robustly by both in-situ ground monitors, such as the Aerosol Robotic Network (AERONET), or by remote-sensing tools such as satellites or aircrafts. Whilst AERONET can give comprehensive hourly datasets, satellite imagery is commonly used due to the large spatial coverage it provides. Satellite derived AOD is measured by recording electromagnetic radiation, with the observed distortion of radiation observed on a radiative transfer model being converted to AOD (Kumar *et al.*, 2007). Examples of instruments that measure AOD remotely include the Moderate Resolution Imaging Spectroradiometer (MODIS) onboard NASA’s polar-orbiting satellite TERRA, the Medium Resolution Imaging Spectrometer (MERIS) aboard ENVISAT and, most importantly for this paper, the Sea and Land Surface Temperature Radiometer (SLSTR) on board ESA’s Sentinel 3-A.

Satellite sensors looking down at the Earth’s surface will measure backscattered radiation from aerosols, clouds, and other atmospheric molecules. Figure 1 shows a simple illustration of a remote sensing setup, where θ_0 is the solar zenith angle, θ_s is the satellite view zenith angle, and φ is the relative azimuth angle.

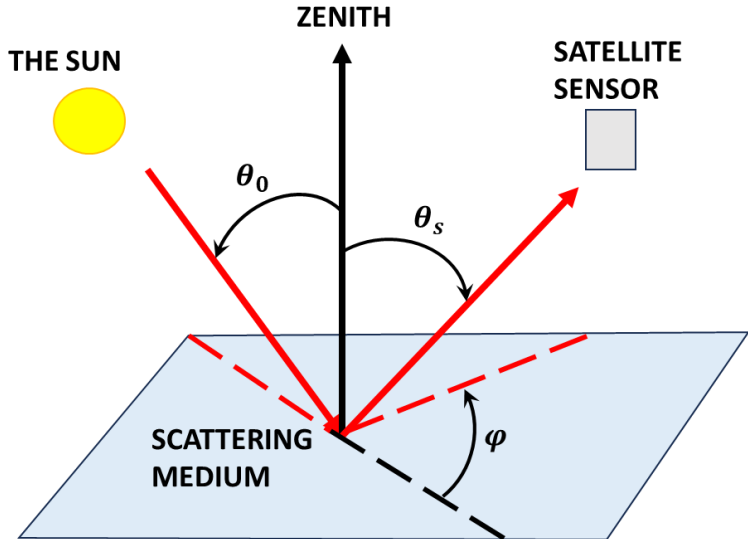


Figure 1: A simple illustration of a remote sensing setup (Kokhanovsky & de Leeuw, 2009).

The observed reflectance consists of backscattered solar radiation, direct and diffuse radiation that the satellite sensor directly receives, and direct and diffuse radiation that the satellite sensor diffusely receives after passing through atmospheric molecules. Depending on how atmospheric aerosols are backscattered, the aerosol retrieval and spectral signals will be different. Different wavelengths of radiation and view angles need to be utilised in order to estimate the aerosols. Most aerosol retrieval schemes return spatially varying estimates of AOD at the main parameter, with the main challenge of satellite aerosol retrieval after cloud filtering is the separation of aerosol scattering and land surface reflectance, especially over bright surfaces.

The majority of available aerosol retrieval datasets are from instruments that have single-view sampling. These views rely on *a priori* knowledge, or theoretical deductions, of the spectral properties of the surface in order for an algorithm to separate the aerosols and the surface contributions. The retrieval algorithms, and the choice there of, are the main sources of uncertainty in AOD measurements. Multiple methods have been utilised in the past, including dark target retrieval; where patches of dark vegetation are identified, as there are known spectral properties,

that can then be used to derive aerosols over these targets. Meanwhile, other instruments employ spectral mixing algorithms, where a surface spectrum is derived from a linear combination of in-situ measurements. Spectra of vegetation and bare soil are taken, and then an algorithm sorts through light and dark pixels in order to determine vegetation cover and assumes atmospheric information to be constant. Whilst this process will produce good results in areas where the assumptions are correct, there may be a large number of uncertainties on a global scale. MODIS is an example of a single-view instrument that uses an operational algorithm with dark target retrieval. Whilst MODIS has a higher global daily coverage, due to its larger swath width, there are disadvantages. There is a low number of MODIS observations over bright surfaces, such as cities or agricultural areas, such as the city of Hamburg in northern Germany.

These uncertainties can, however, be reduced by using an instrument that has multiple views. Dual-view methods show robust retrievals for both bright and light surfaces, a notable advantage over instruments such as MODIS. In the along-track direction, the shift in the observation scene as the satellite orbits causes the two viewing observations to have juxtaposed scenes at ground level, referred to as the parallax effect. This parallax effect is used to find aerosol layer height. Multiple-view angle approaches do not require any *a priori* information of the spectral surface or surface albedo, and the observation capability enable the properties of the Earth's surface to be better characterised. This allows top of the atmosphere (TOA) radiance to be separated into surface aerosol and aerosol scattering. SLSTR, which is onboard Sentinel-3, is one such example of a dual-view instrument and differs in terms of aerosol retrieval algorithm in comparison with MODIS.

2.1.2.1. SLSTR onboard Sentinel-3A AOD

The Sentinel-3 satellites have a near-polar, sun-synchronous orbit, crossing the equator at 10:00 mean local solar time. On board both Sentinel-3a and Sentinel-3b are the SLSTR instruments, which are dual-view conical imaging radiometers that are, as previously mentioned, evolved from the AATSR sensors. Being an along-track scanning dual-view instrument means that the same scene is measured twice. Compared to the AATSR sensors, SLSTR has an extended swath width of 1420km in nadir view, and a 750km swath in the off-nadir or oblique view, with a 55°zenith angle. Figure 2 shows a simple illustration of SLSTR's dual-view configuration. The SLSTR instruments have a mean altitude of 815km. The combination of the two satellites allows for global revisit times of 0.9 days at the equator, or 1.9 days with only one, with a 27-day repeat orbit and a 4-day sub-cycle. There are 385 orbits per cycle. The retrieval of aerosols is exclusively achieved in the daytime, with only solar zenith angles lower than 80°considered. SLSTR collects reflectance data in nine spectral bands in the 0.5–12 µm spectral range, detailed in table 7.

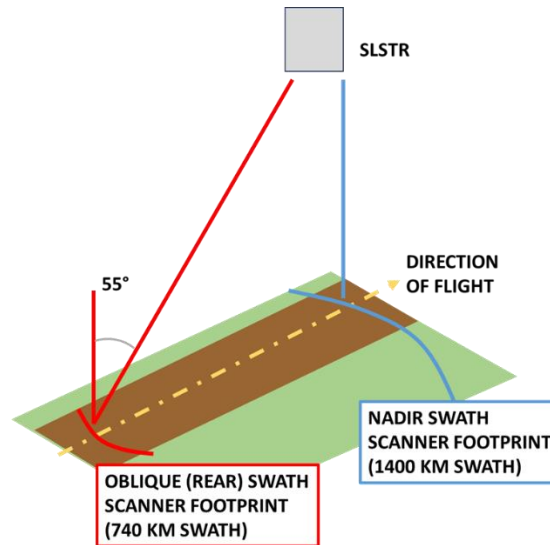


Figure 2: Schematic view of SLSTR dual-view configuration (Donlon et al., 2012)

Table 7: Wavelengths for the SLSTR instrument

Channel	Wavelength (nm)	Bandwidth (nm)
1	554	20
2	659	20
3	868	20
4	1375	20
5	1613	60
6	2255	50
7	3742	398
8	10854	776
9	12022	905

SLSTR aerosol retrieval is derived from multi-angular observations, using a linear weighted combination of a geometry method, which combines the dual-views, and a spectral method that derives the spectral reflectance of each view. As discussed previously, instruments with multiple view-angles allow for a more robust retrieval of aerosols, even over bright surfaces. The best AOD performance, using the 550 nm wavelength band, is obtained mostly on the half Eastern side of both the nadir and oblique swaths for all latitudes in the winter months, and the southern latitudes for the summer oblique swaths.

SLSTR aerosol retrieval is of variable quality, with preliminary regional validation with AERONET showing high correlations over polluted areas, with a multitude of factors that can cause uncertainties when deriving AOD. Aerosol scattering variability represents the greatest uncertainty in the derivation of surface reflectance in remotely sensed datasets, the magnitude of which increases with view angle. One of the most significant challenges of dual-view sensors is that due to the limit of two views there will only be a certain range of scattering angles no matter what orientation the satellite is in. This means that some areas of the Earth will always be measured with backscattering, whilst other areas will have both backscattering and forward scattering samples. Out of the two views there are higher uncertainties in the oblique backscattering direction, so corrections need to be applied when using the off-nadir view of SLSTR datasets. Additionally, corrections need to consider both geometry and spectral constraints to ensure overall quality. SLSTR datasets have higher uncertainty over urban soils and unfavourable geometry due to inaccurate

spectral coefficients. Unfavourable geometry tends to occur in the north during the summer and the western side of the nadir and oblique swaths in the winter.

The datasets used in this study may also have significant limitations. There may be artificially low AOD measurements due to incorrectly screened night-time granules. Unfiltered cloud residuals, on the other hand, may lead to high AOD outliers. The SLSTR datasets used in this study may not have been comprehensively validated by EUMETSAT before they were released on open access, as the data was processed before the EUMETSAT validation report was published. SLSTR AOD is limited in terms of spatial resolution because of the smaller scan width (Hands Schuh *et al.*, 2022).

Over land, the algorithm employs a parameterised model of the surface angular anisotropy and uses the dual-view capacity to allow surface spectral reflectance without assumptions. The key features of the algorithm are summarised in chapter 3 and are expanded upon in detail in the Algorithm Theoretical Basis Document (North and Heckel, 2019).

2.2. Current Research

2.2.1. Correlation

PM_{2.5} and AOD correlations can have massive variations, particularly spatially, and the values found are sometimes not statistically significant. This is because the accuracy of the correlation depends on the aerosol source region, and chemical characteristics (Kumar, Saxena and Yadav, 2011). The studies performed are representative of this, as linear regression functions and their associated correlation coefficients displayed significant variations depending on the study region. This is due to the differences between PM_{2.5} and AOD in terms of what aerosols are included in their datasets. PM_{2.5} represents the aerosol mass at the ground, and additionally often only measures the dry mass concentration of fine particulate matter, excluding the presence of water vapour and coarser particles such as pollen (Yang *et al.*, 2019). AOD, on the other hand, represents the whole atmospheric column and contains all types of aerosols, as it looks at the total atmospheric column's radiation extinction ability and water vapour increases the value of AOD. Hence, additional factors such as relative humidity, aerosol source, planetary boundary height and vertical distributions may need to be considered (Zheng *et al.*, 2017; Zhang and Li, 2015).

Satellite-derived correlations of PM_{2.5} and AOD have the potential to measure PM variability with a much higher spatio-temporal resolution and coverage than ground stations (Schneider *et al.*, 2020). A significant amount of the literature shows strong correlations between PM_{2.5} and AOD (Wang and Christopher, 2003). From these studies, linear regression is the primary method used, and has been found to be more accurate than using daily mean values as a comparator (Kong *et al.*, 2016).

Yang *et al.* (2019) found a high correlation in the densely populated BTH and Chengyu regions of China, which have high concentrations of fine particles due to predominantly urban industry emissions. Schneider *et al.* (2020) found that their overall cross-validated R^2 values ranged from 0.704 to 0.821, with an average of 0.767. There was an average prediction error of 4.042 $\mu\text{g m}^{-3}$. These values line up well with other studies, with Shi *et al.* (2018) using land use regression modelling to find an uncalibrated correlation of $R^2 = 0.07$ and a calibrated correlation of $R^2 = 0.72$, Yang *et al.* (2019) finding a R^2 values of 0.89 in 2014 and 0.73 in 2017, and Wang *et al.* (2019) using the linear mixed effect model and MODIS AOD discovering a strong correlation of $R^2 = 0.78$ over BTH. Kong *et al.* (2016) used linear regression to compare MODIS AOD and PM_{2.5} in Beijing, China and found that the linear regressions varied from $R^2=0.58$ to $R^2=0.55$ to $R^2=0.64$ in the city, suburban region, and background respectively. All correlations were positive, with slopes ranging from 20 to 120 in the regression functions and the RMSE varying from 8% to 33% in urban regions and the background respectively and the study found that the PM_{2.5} values that could be retrieved by these

correlations were more rational when taken from polluted areas. Other studies looked at the correlation in terms of changes, with Kumar *et al.* (2007) finding that a 1% change in AOD explained $0.52 \pm 0.202\%$ and $0.39 \pm 0.15\%$ of $PM_{2.5}$ changes monitored within ± 45 and 150 min intervals of AOD data, which is a significant positive association. Kaskaoutis *et al.* (2010) used linear regression with MERIS AOD and discovered that the 560nm band was found to be the best correlated wavelength, with the highest slope and the lowest intercept. This study posits that the strong positive correlation between satellite derived AOD and ground based $PM_{2.5}$ means that the majority of aerosols were found within the planetary boundary layer and was statistically significant at 95% confidence level.

Conversely, Standgren *et al.* (2014) found negative correlations when investigating the correlation between AOD and $PM_{2.5}$ in the United States, particularly in Salt Lake City. This study observed the wildly differing correlations even within the United States and found that it was heavily dependent on both surface and atmospheric conditions. Atmospherically elevated haze from fires and dust were attributed to being one potential cause for the negative correlation, as satellite derived AOD only describes the total measurement within an atmospheric column, with no vertical variation. Fine mode fraction is another potential cause, where the low fine mode fraction value found in Salt Lake City may indicate coarse particles found in the AOD dataset that is not in the $PM_{2.5}$ data. Yang *et al.* (2019) also found low concentrations in coastal areas due to this reason, because the AOD types in these regions are mainly sea salt, dust, and water vapour, when the main sources of $PM_{2.5}$ come from fossil fuel emissions.

This latter point demonstrates that the correlation between $PM_{2.5}$ and AOD is affected by many different factors, as previously discussed. $PM_{2.5}$ and AOD sometimes have weak correlations when the meteorological conditions are different. Yang *et al.* (2019) found that high humidity increased the water content of the aerosols, which only increased AOD values, and Kim *et al.* (2019) found that as relative humidity decreased so did the correlation. Shi *et al.* (2018) noted that meteorological variables need to be considered, both building upon the previously discussed points, and additional ones such as seasonal changes and microclimates. Standgren *et al.* (2014) found poor correlations except for July, which was most likely due to better atmospheric conditions such as a lower relative humidity and a higher boundary layer height combined with pollutant events such as wildfires and smoke.

These factors lead to significant spatial variations. Van Donkelaar (2006) found a wide range of correlation coefficients between different cities, with stronger values of 0.67 and 0.35 in Toronto, to a weak correlation in Washington of 0.09 and -0.11 in MODIS and MISR respectively. Tian and Chen (2007) however found massively different correlation coefficients between stations within the same city, with correlations of -0.119, 0.235, 0.748 and 0.637 at Toronto East, West, North and South respectively. It should be noted that the major industrial pollution sources are found in the East and West. Lalitaporn and Mekaumnaychai (2020) also found that the regression analysis performed better over oceans than land, with correlation coefficients of 0.72-0.83 and 0.57-0.79 respectively. Standgren *et al.* (2014) discovered negative correlations at Salt Lake City and Phoenix, which were likely due to atmospherically elevated haze. The negative correlations may also be attributed to the fine mode fraction, with Salt Lake City having coarser particles, such as salt particles from the nearby salt flats, than Atlanta, one of the other study sites that had a positive correlation. This notion that correlations can be weaker in coastal areas is backed by multiple studies (Yang *et al.*, 2019; Xin *et al.*, 2016). Standgren *et al.* (2014) also notes that the correlations increase with increased AOD spatial resolution yet decrease with an increasing scale of the study region, and a low variability of AOD can lead to reduced correlation especially at a higher spatial resolution where uncertainty is increased. Shi *et al.* (2018) validated this notion, showing that distinct variations between districts in ground measured datasets can heavily affect the correlation. With an increased study area, the variations in

the PM_{2.5} datasets would average out, and this would decrease the correlation, but with a more specific study with high resolution data, the correlation would be stronger.

Additionally, temporal variations occur in the correlations. Tian and Chen (2007) found their study's correlation is far stronger in summer than winter, with a summer correlation of 0.575 and a winter correlation of 0.103. Yang *et al.* (2019) and Paciorek *et al.* (2008) backed up this claim. Kong *et al.* (2016) however found the opposite of this phenomenon, with the summer minimum value being half of the winter maximum value, which Xu *et al.* (2021) and Kim *et al.* (2019) agreed with. There are also variations within the day. Xu *et al.* (2021), who studied the correlation in 345 cities and 14 urban agglomerations, found the correlation had the strongest relationship at noon and in the afternoons, and was markedly stronger in the day than at night. Standgren *et al.* (2014), using MODIS AOD, also found seasonal variability, with the lowest correlation coefficient of 0.143 occurring in the winter and the highest of 0.587 occurring in the summer.

There have been many studies that have looked at improving the correlations and reducing the errors found. Xu *et al.* (2021) found that the correlation is stronger between PM_{2.5} and fine mode AOD and is even stronger when daily measurements are used. Xin *et al.* (2014) agreed with this, as through their study comparing the correlations of both ground and MODIS AOD to PM_{2.5}, which found the same correlation coefficient of 0.75, they discovered the main cause of error was monthly aggregation and seasonal variations.

Whilst there is a knowledge gap present in correlations between satellite derived AOD data, such as from Sentinel-3A, and ground measured PM_{2.5}, due to a current lack of studies in this area, there has been research made into correlations between other satellite-derived AOD and PM_{2.5}. There has been a wide variety of correlations found between studies.

2.2.2. Current Limitations

Recent research has highlighted the need for an improved understanding of atmospheric processes. Wang *et al.* (2020) noted that the role of chemistry and meteorology was not understood in looking at the spread of emissions and aerosols, with Zielinski *et al.* (2016) noting that the lack of direct quantification of global distribution and turbulent mixing causes a lot of uncertainty, and with Conticini *et al.* (2020) looking at how this would affect the stagnation of pollutants. Wang *et al.* (2003) inferred that during cloud-free conditions, which are often needed in satellite observations, the boundary layer is well-mixed, which may result in stronger correlations.

There are also not many research groups that run complex atmospheric chemical models, hence small-scale variability is still difficult to model (Zielinski *et al.*, 2016., Sheel *et al.*, 2019). Wang *et al.* (2019) also found that there has hardly been any research into combining ground measurements, atmospheric chemical models, and satellite observations. The correlation between these has not yet been fully explored, with studies such as Schneider *et al.* (2020) finding limitations in the sense that satellite-derived AOD does not represent the surface values that ground-measurements would give, but the total atmospheric column concentrations. The scarcity of PM_{2.5} monitoring has also contributed to lower correlations. Models are often generalised spatially, and the selected location of ground-based stations may not be fully representative of the full study location. Standgren *et al.* (2014) noted that the relationship between AOD and PM_{2.5} is still poorly misunderstood when considering spatial resolution. Whilst a higher spatial resolution allows for a much larger investigation, errors such as cloud contamination can have a much larger effect on the AOD quality.

2.3. Conclusions

This review of recent and important literature demonstrated the importance of studying air quality. This is to protect public health, the economy, and prevent environmental changes. Regional and

seasonal variations were also repeatedly found, depending on where the study took place, the spatial resolution of their datasets, whether meteorological parameters such as relative humidity and temperature were factored in, and what timescale was considered. Something that is also of note is that most of the literature sampled used MODIS, with only a few using other datasets such as AERONET. No literature using Sentinel-3a AOD was found. This reinforces the motivation for this study, to investigate whether Sentinel-3a is comparable to AERONET correlations at all.

3. Methodology

To achieve the goal of this thesis, which is to compare the correlations of $PM_{2.5}$ and AOD using two different AOD retrieval methods, several different datasets have been collected and used. This research paper uses secondary data collected from January 2017 to December 2020 for the monthly averages. The rationale for collecting data for the 2017 to 2020 period was to have at least three stable years of air quality data. Due to the COVID-19 pandemic, there were fluctuations in air quality during 2020, particularly in the first few months of the year. 2020 was henceforth included within the study period in order to determine how sensitive both Sentinel-3a AOD datasets and the subsequent $PM_{2.5}$ correlations are to air quality changes.

3.1. Study Regions

This study looked at the correlations between $PM_{2.5}$ and AOD at the city-scale, meaning that ground measured $PM_{2.5}$ datasets from within certain cities were collated, and correlated against matching gridded Sentinel-3a AOD or AERONET stations. The cities needed to have data available for the above time periods for $PM_{2.5}$, Sentinel-3a AOD and AERONET AOD.

In total, six cities were studied. These are Beijing, Houston, Los Angeles, New York, Mexico City and Torino. Four of the cities that were investigated are in North and Central America, one is in Asia, and one is in Europe.

3.2. Satellite Datasets

3.2.1. Sentinel-3A AOD

In this study, satellite derived AOD was taken using the SLSTR instrument on board Sentinel-3a. Specific details of the SLSTR instrument, including the orbit and spectral bands, are included in Chapter 2 of this thesis. Only Sentinel-3a data was used as Sentinel-3b data was launched halfway through the study period. Sentinel-3a AOD data was downloaded from the Copernicus Climate Data Store (<https://cds.climate.copernicus.eu/cdsapp#!/dataset/satellite-aerosol-properties?tab=overview>). Whilst SLSTR data can have a spatial resolution of 500m, the available data from the Climate Data Store is presented on a $1^\circ \times 1^\circ$ lat-long grid, so with a much larger spatial resolution than the base imagery SLSTR can provide. This is a known limitation of this study, as a larger spatial resolution would be able to show much more variation on a city-scale. However, this limitation may be offset by the reduced risk of introducing errors such as cloud screening. A coarser resolution may overcome the theoretical advantage if the introduced error in a high-resolution dataset is too high. In the dataset used, one pixel would correspond to a city. In order to do a correlation with ground-measured $PM_{2.5}$, as ground-measured $PM_{2.5}$ only measures the aerosol concentration in the immediate vicinity of the station, $PM_{2.5}$ datasets need to be aggregated across the AOD pixel.

The best performance of SLSTR AOD, using the 550nm band as a reference, is in the southern latitudes with oblique swaths. There appears to be a good correlation of SLSTR AOD with MODIS and AERONET, with higher correlations seen in more polluted areas such as Asia, Australia, and South America, with Europe seeing lower correlations. Whilst the advantages of satellite based AOD observations very importantly include global coverage, there are drawbacks. Known limitations of SLSTR AOD retrieval include the underestimation of AOD values in areas of low aerosol pollution or complex topography, and the overestimation over bright surfaces such as deserts. Cloud coverage remains a significant limitation as unfiltered residuals can lead to high AOD outliers, and in some cases is the cause of missing data. Unfavourable geometry can also cause high uncertainties and positive biases for low AOD values. Dual-view sensors have the additional restriction of having a limited scattering angle range, requiring extra calculations so that AOD retrieval remains consistent.

3.2.1.1. Algorithm Outline

The data used was SLSTR-3A for the period 01-07-2017 to 31-12-2020. The data were processed at the UK's Jasmin environmental science data processing facility, with data made available from the European Space Agency. The algorithm that was used to retrieve and compile the AOD datasets was developed by Peter North and his team from Swansea University (North and Heckel, 2019). The aim of the algorithm is to make use of both the angular and spectral sampling available from SLSTR. For 5 solar retrievals reflective SLSTR bands, using both nadir and oblique views and geometry, location and pixel identification information, aerosol optical depth of a reference wavelength will be outputted. Additionally, estimates of aerosol fine mode fraction, absorption and spectral dependence can also be calculated.

The algorithm requires screening of input pixels to remove unsuitable pixels. This includes clouds, sun glint, snow, and ice pixels. Each pixel that is flagged as being unsuitable is removed, as well as all 8 of the direct pixel neighbours as they are considered contaminated. Pixels are screened for both nadir and oblique views. Then the pixels are aggregated into super-pixels, or a 9x9 grid of pixels at 500m spatial resolution, with the centre pixel being responsible for parameters such as geo-location and geometry. Super pixel resolution is 4.5km x 4.5km. If more than 50% of the pixels within the super pixel are considered valid, then the super-pixel will also be valid for AOD retrieval. Then, surface reflectance is derived from an atmospheric radiative transfer model in order to gain knowledge of surface conditions. Look up tables (LUT's) are pre-compiled for candidate aerosol models, in order to represent a variety of aerosol types. This allows for TOA reflectance to be calculated. TOA reflectance is the input to the algorithm, with the resolution of the super pixels being appropriate to minimise errors. Surface reflectance is calculated for a given atmospheric aerosol model, with AOD being parameterised by value. The data is subject to constraints such as geometry and bright surfaces.

3.2.1.2. Data

Sentinel-3a datasets were downloaded in netCDF format, and were viewed in Panoply, which is a freely-available geo-referenced data plotting tool from NASA Goddard Space Flight Center that creates images such as figure 3. Figure 3 shows a monthly average of Sentinel-3a data.

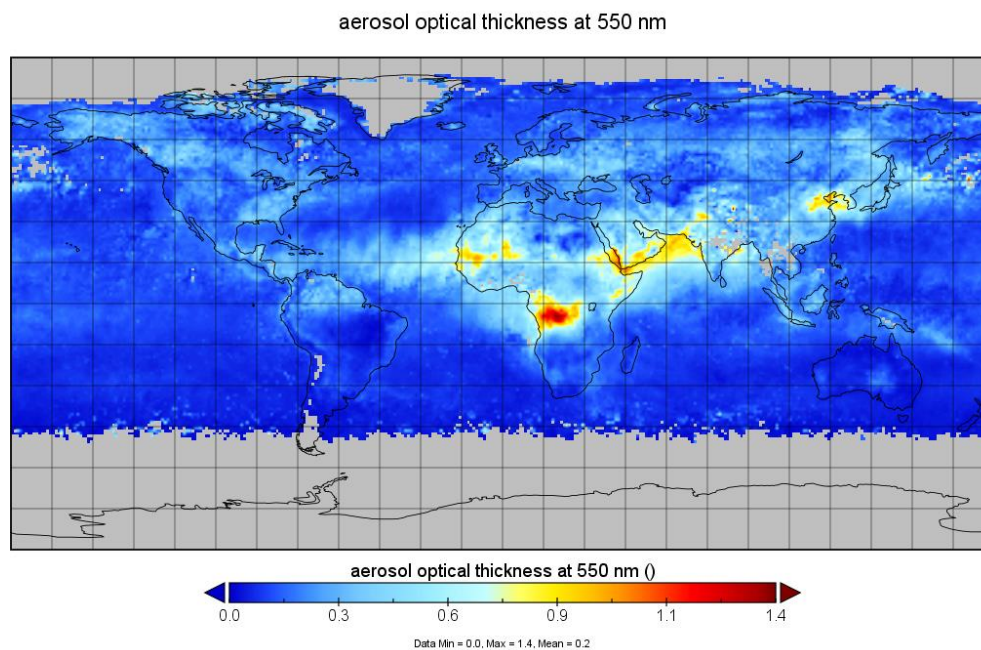


Figure 3: Example image of what Panoply looks like for a monthly average of Sentinel-3a AOD

In order to derive AOD from Panoply, we would need to go into the gridded dataset. The Sentinel-3a dataset used was a 1° x 1° lat-long grid, meaning that there would be a grid of data to correlate to the city being studied. Figure 4 shows what this looked like.

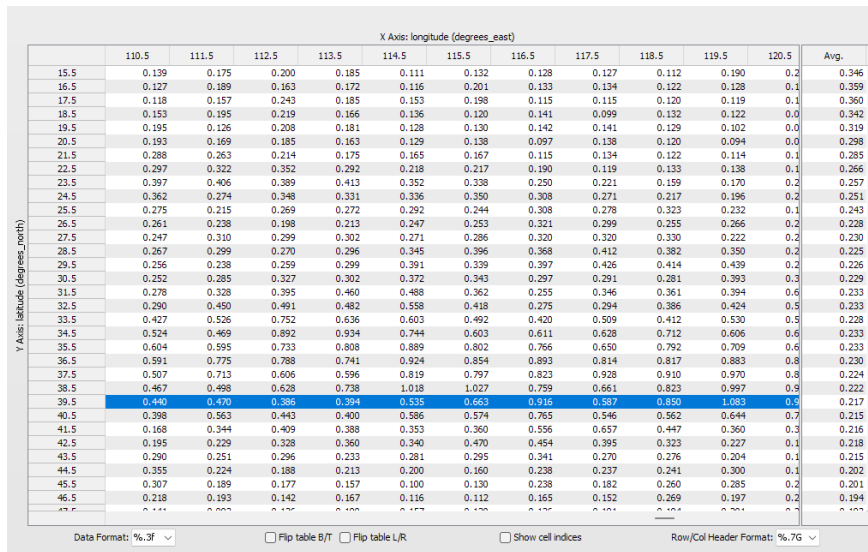


Figure 4: Example image of Panoply

For each city being studied, a pixel from the lat-long grid was used. The AOD value found in this pixel corresponds to the aggregate, average AOD value for this location. Table 8 shows which pixels were used to obtain Sentinel-3a AOD datasets, with the latitude and longitude referring to the centre coordinates of the lat-long grid.

Table 8: Table showing which grids were used to obtain Sentinel-3a AOD data.

	Latitude	Longitude
Beijing	39.5	115.5
Houston	29.5	-95.5
New York	40.5	-74.5
Los Angeles	33.5	-117.5
Torino	44.5	7.5
Mexico City	18.5	-98.5

3.3. Ground Datasets

3.3.1. PM_{2.5} Datasets

This research paper utilised daily PM_{2.5} data obtained from a variety of different sources. All of these sources appear to be comparable in terms of the instruments used, though may vary slightly in accuracy due to the change in location. All of the PM_{2.5} data, no matter what source, were downloaded in an hourly format. The datasets would vary in frequency however, as some instruments would not record data for periods of time. Table 4 shows which sources were used to gather PM_{2.5} data.

Table 9: Table showcasing the PM_{2.5} sources

Country	City	2017	2018	2019	2020	Source	Download Source
Australia	Sydney	JULY-DEC	ALL	ALL	ALL	NSW Department of Planning, Industry and Environment	https://openaq.org/#/countries/AU
China	Beijing	JULY-DEC	ALL	ALL	ALL	China National Environment Monitoring Centre	https://openaq.org/#/countries/CN
Italy	Torino	JULY-DEC	ALL	ALL	ALL	European Environment Agency	https://discomap.eea.europa.eu/map/fme/AirQualityExport.htm
Mexico	Mexico City	JULY-DEC	ALL	APR-OCT	APR-OCT	https://www.airnow.gov/	https://openaq.org/#/countries/MX?page=1
USA	Houston	JULY-DEC	ALL	ALL	ALL	https://www.airnow.gov/	https://openaq.org/#/countries/US
USA	Los Angeles	JULY-DEC	ALL	ALL	ALL	https://www.airnow.gov/	https://openaq.org/#/countries/US
USA	New York	JULY-DEC	ALL	ALL	ALL	https://www.airnow.gov/	https://openaq.org/#/countries/US

One of the main sources used was openaq.org, which is a non-profit organisation that collates PM_{2.5} from multiple governmental sources. Each file is readily downloadable in an excel compatible document. For each city, the data from a variety of PM_{2.5} stations were downloaded and aggregated into firstly a city-wide average, and then averaging out the hourly data into monthly data.

Table 10: PM_{2.5} stations that were aggregated for this study, and their respective latitude and longitudes.

Country	City	Location ID	Location Name	Latitude	Longitude	
Italy	Torino	IT0470A	IT0470A	45.10407	7.69534	
		IT2168A	IT2168A			
		IT1877A	IT1877A			
USA	Houston	162	Houston Deer Park C3	29.67003	-95.12851	
		191	Seabrook Friendship	29.5831	-95.0156	
		1220	Galveston Airport C1	29.2631	-94.8564	
		186	Houston Aldine C8	29.9011	-95.3261	
	New York	626	Bronx - IS52	40.8161	-73.9022	
		928	Jersey City FH	40.72545	-74.05229	
		665	Bronx - IS74	40.8147	-73.8867	
		662	Division Street	40.7142	-73.995	
		857	Fort Lee Near Road	40.85355	-73.9661	
	Los Angeles	628	Maspeth	40.7269	-73.8933	
	847	South Long Beach	33.79222	-118.1753		
	Mexico	Mexico City	2006	FES Aragon	19.4525	-99.086
			1791	Merced	19.4246	-99.1195
2020			San Agust�n	19.5329	-99.0303	
1659			Tlalnepantla	19.529	-99.2045	
2054			Nezahualc�yotl	19.3919	-99.0281	
1986			Santiago Acahualtepe	19.3502	-99.1571	
China	Beijing	21	Beijing US Embassy	39.95	116.47	
		10134	10134	39.8863	116.4072	
		9820	9820	39.9289	116.4174	
		9087	9087	39.9934	116.315	

		10041	10041	39.9136	116.184
		7589	7589	39.9821	116.3966
		10167	10167	39.9295	116.3392
		9792	9792	39.8784	116.3621

3.3.2. AERONET AOD

The Aerosol RObotic NETwork, or AERONET, is a ground-based network that monitors local aerosol properties. Active since 1993, the NASA Goddard Space Flight Centre has a historical record publicly available for over 800 sites. AERONET uses sun photometers, which takes measurements every 15 minutes. AERONET is a robust, long-term, and openly accessible database, which is accessible from https://aeronet.gsfc.nasa.gov/cgi-bin/webtool_aod_v3. All the cities used in this study had at least one AERONET station present, with Beijing having 5 that were usable, and hence they were averaged out. To compare the AERONET AOD values to Sentinel-3a, 870nm and fine mode AOD were extracted from the download, and the AOD at 550nm was calculated using the Ångström parameter (how AOD changes with wavelength, and is related to particle size).

3.4. Methods

After original raw data was downloaded from the respective sites, data was collated into Microsoft Excel. Sentinel-3a was manually inputted into an excel document after visualising the netCDF file in Panoply, and the PM_{2.5} datasets and the AERONET datasets were present in a csv file format. Once all of the datasets were in an excel file, they were aggregated into monthly values. These were then plotted against one another in order to determine the linear regression. Both of the AOD datasets are the primary independent variable of this study.

4. Results

In this chapter the results of the thesis will be presented. This chapter is split into two major sections. The first section will deal with the aggregated monthly $PM_{2.5}$ data and the correlations with both Sentinel-3a AOD and AERONET AOD for the 2017-2020 period. This section will also look at the differences in correlations between the 550nm AOD, 870nm AOD, and fine mode AOD with $PM_{2.5}$. The results will be shown using both tables and scatter plots. The tables contain statistical information about the linear regression, such as the R^2 value, the slope and the intercept.

4.1. Monthly Correlations

4.1.1. Correlation between $PM_{2.5}$ and Sentinel-3a with comparisons to AERONET AOD

This subsection will focus on both investigating the performance estimating $PM_{2.5}$ datasets using Sentinel-3a AOD datasets for each of the six cities investigated. Additionally, there will be a global scatter plot presented, which is all of the points from the six cities presented onto one graph. This subsection will be split by the three AOD wavelengths that were looked at for the monthly correlations, showing the linear regression graphs of Sentinel-3a correlations, followed by the AERONET correlations. This subsection will end with a comparison table, where the performances of each wavelength and instrument will be discussed.

4.1.1.1. 550nm

Figure 5 shows the aggregated Sentinel-3a AOD and corresponding $PM_{2.5}$ concentrations for the period July 2017 to December 2020, presented using scatter plots. Examining the global average first, there is no correlation between the two measurements, with an R^2 value of 0.0036. The linear regression model has a slope of -10.483 and an intercept of 21.649, so a slight negative correlation. The majority of points are distributed in the bottom-left corner of the graph, with low $PM_{2.5}$ values on the Y-axis that gradually increase with increasing AOD. However, there are numerous outliers, particularly in the top-left quadrant, with what would be considered dangerously high $PM_{2.5}$ concentrations coinciding with relatively low AOD. There are also a considerable number of points in the bottom-right quadrant, with high AOD values measured against lower numbers of $PM_{2.5}$. What this global graph doesn't show is just how much the correlation varies between cities. The R^2 values vary from a maximum of 0.2848 in Torino, to a minimum of 0.0273 in Beijing. Interestingly, the slopes varied from -94.714 in Torino, to 23.886 in Los Angeles, meaning that the correlation between AOD and $PM_{2.5}$ can be negative. There is no consistent pattern with the slopes and intercept, showing that the correlation very much is location specific.

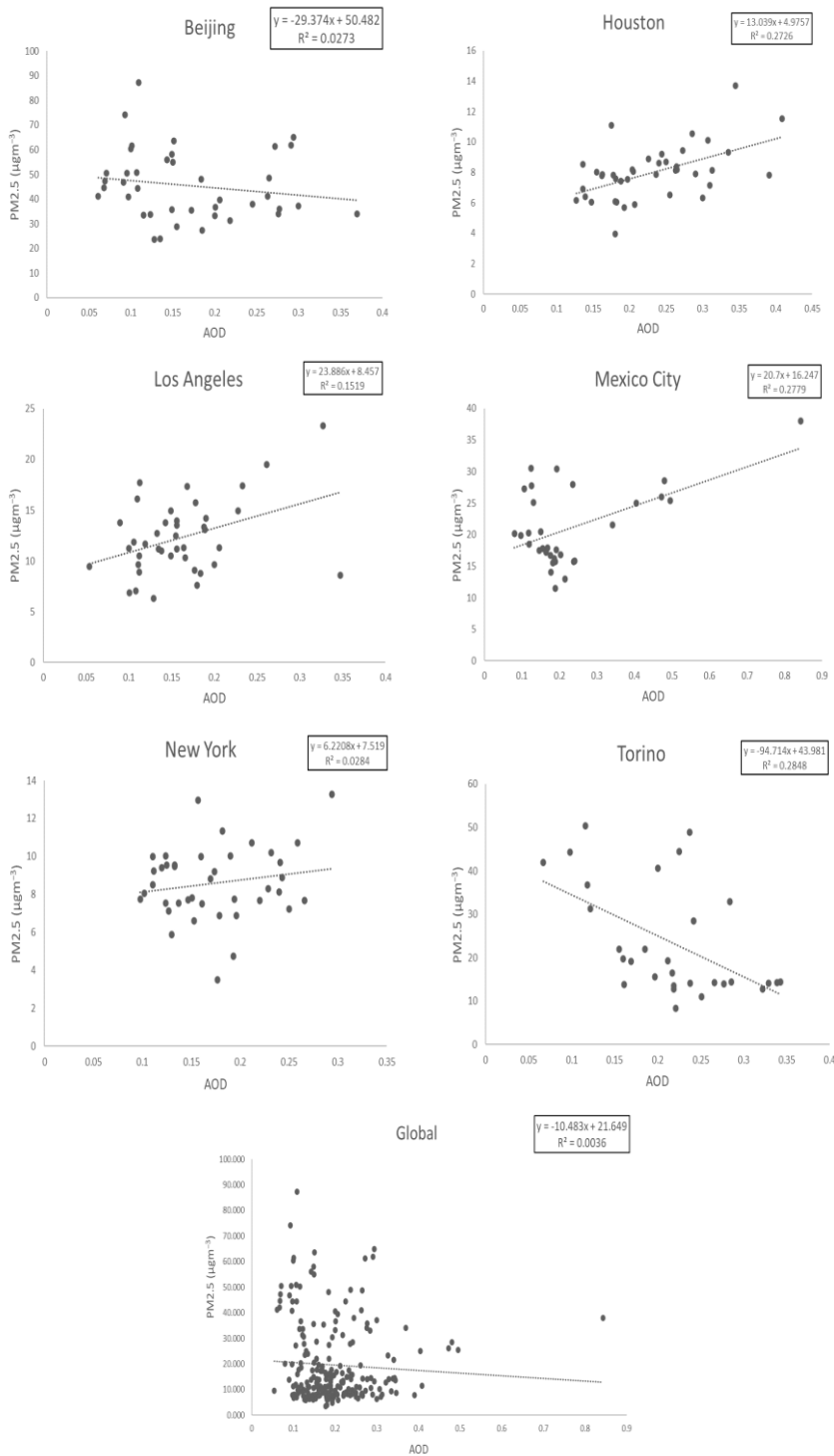


Figure 5: Linear relationship between Sentinel-3a AOD, using the 550nm wavelength band, and PM_{2.5} for a variety of cities. In order, Beijing is upper left, Houston is upper right, Los Angeles is middle left, Mexico City is middle right, New York is lower left, Torino is lower right, and a global dataset of all the points of each of the six cities put on a single graph is at the bottom.

In comparison, Figure 6 shows the monthly aggregated AERONET AOD and the correlation against PM_{2.5}. The global correlation shows a significantly stronger correlation AERONET AOD and PM_{2.5} when compared to the Sentinel-3a correlations, with a positive trend and an R² value of 0.492. The linear regression model has a slope of 69.865 and an intercept of 5.79, so a much steeper trendline. There is a much higher concentration of points in the very bottom left of the global graph, as it looks like AERONET detected lower concentrations of AOD. The best performing correlation was in

Houston, with an R^2 value of 0.5115, and the lowest value was found in New York with 0.0177. The cities also varied massively in slopes and intercept.

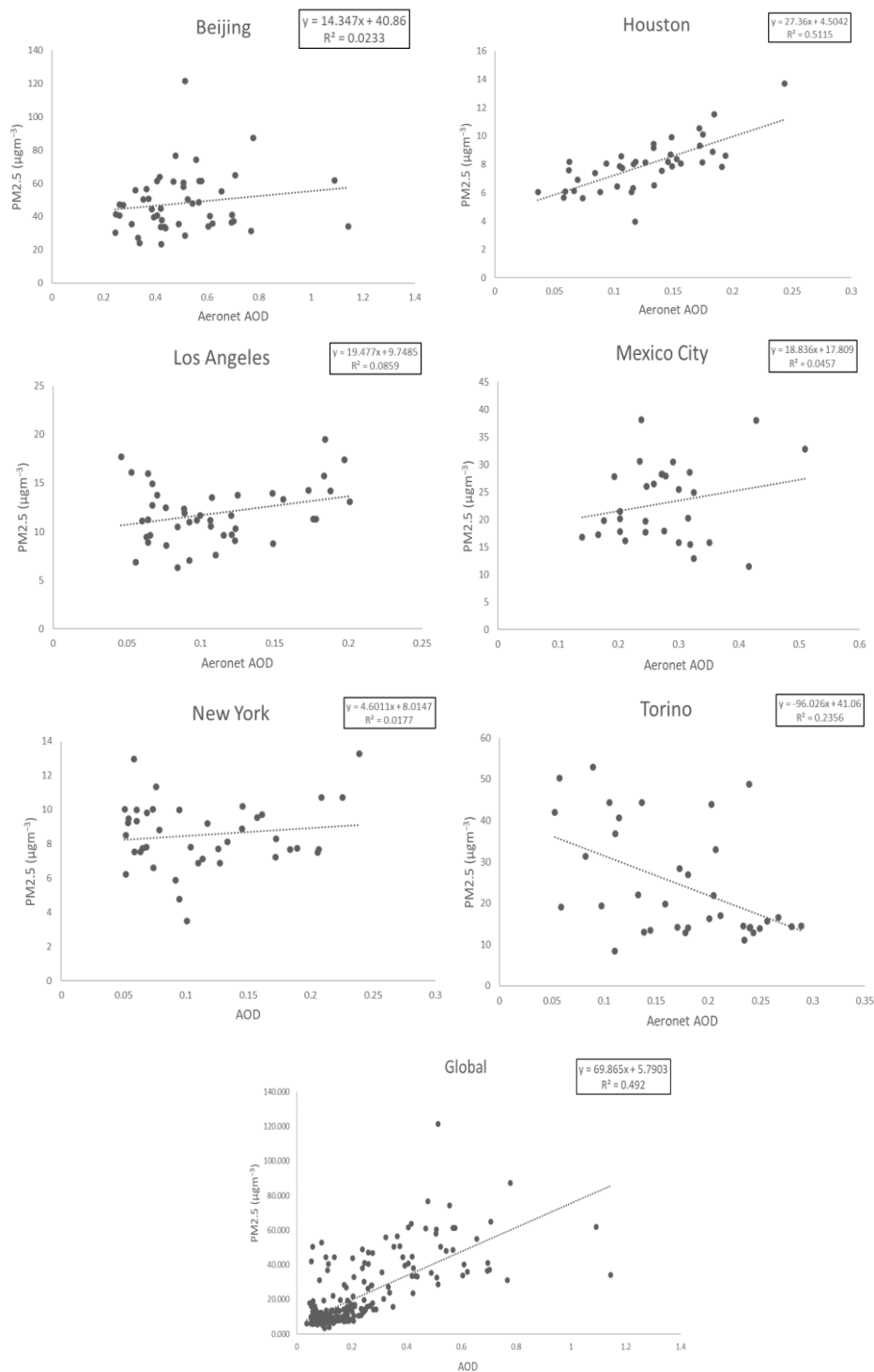


Figure 6: Linear relationship between AERONET AOD, using the 550nm wavelength band, and PM_{2.5} for a variety of cities. In order, Beijing is upper left, Houston is upper right, Los Angeles is middle left, Mexico City is middle right, New York is lower left, Torino is lower right, and a global dataset of all the points of each of the six cities put on a single graph is at the bottom.

4.1.1.2. 870nm

Figure 7 shows the correlation between PM_{2.5} and Sentinel-3A AOD using the 870nm. In these sets of graphs, the highest R² out of the six cities is Torino, with a value of 0.3734. Mexico City has the

lowest R^2 value, with 0.004. In terms of the collated global graph, there is a R^2 value of 0.1495. This set of graphs also have a wide variety of intercepts and slopes, with the slopes ranging from Torino's -197.54 to Los Angeles' 44.261, with Mexico City and New York having almost flat trendlines with slopes of 9.6846 and 6.193 respectively.

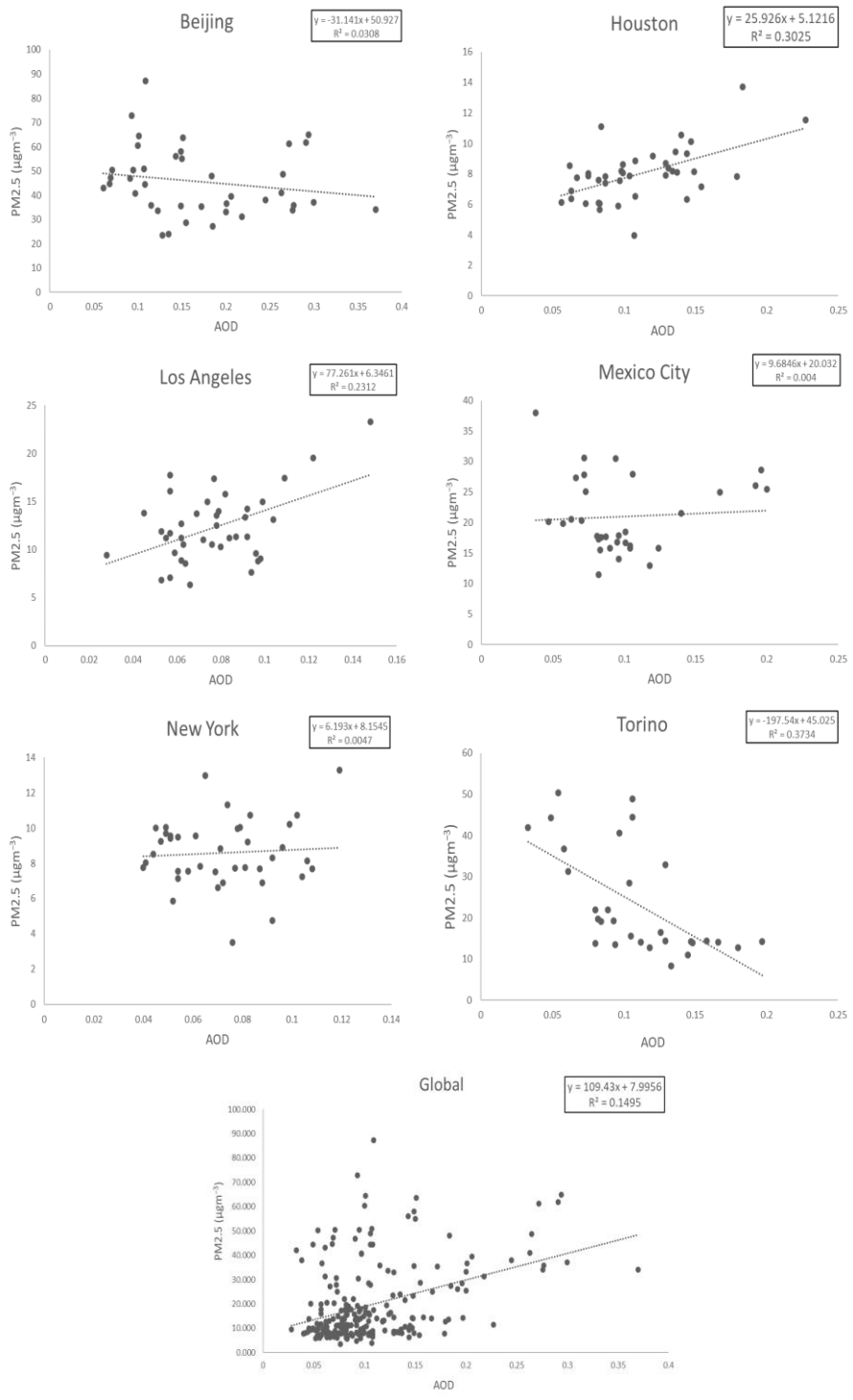


Figure 7: Linear relationship between Sentinel-3a AOD, using the 870nm wavelength band, and $\text{PM}_{2.5}$ for a variety of cities. In order, Beijing is upper left, Houston is upper right, Los Angeles is middle left, Mexico City is middle right, New York is lower left, Torino is lower right, and a global dataset of all the points of each of the six cities put on a single graph is at the bottom.

In comparison, the 870nm AERONET AOD correlations against monthly aggregated PM_{2.5} show similar values. These can be seen in figure 8. The global graph has an R² value of 0.4842, and a strong positive correlation. Houston and Torino have the strongest R² values out of the cities present, with 0.581 and 0.2093 respectively. Houston has a positive correlation and Torino has a negative correlation.

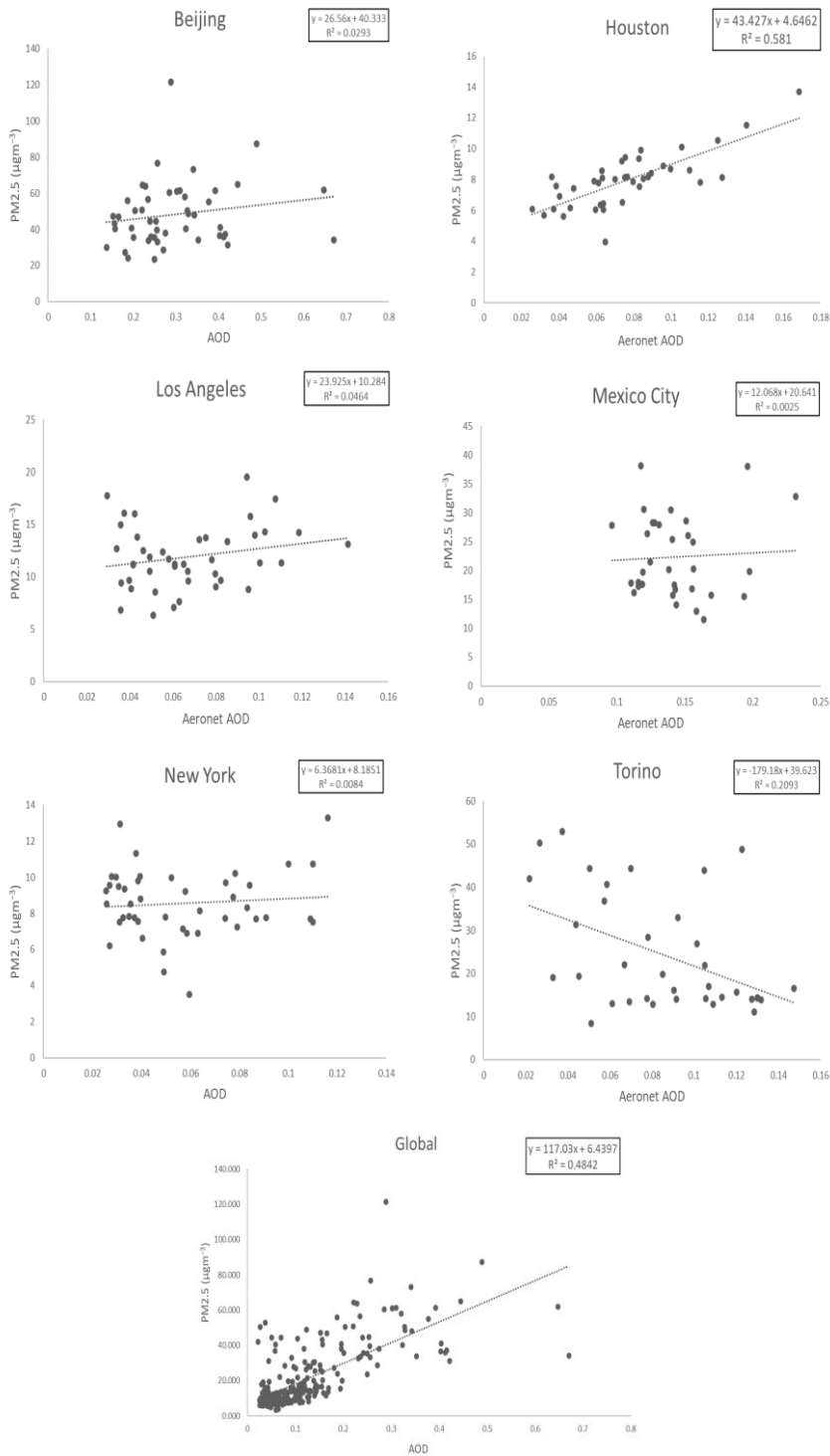


Figure 8: Linear relationship between Sentinel-3a AOD, using the 870nm wavelength band, and PM_{2.5} for a variety of cities. In order, Beijing is upper left, Houston is upper right, Los Angeles is middle left, Mexico City is middle right, New York is

lower left, Torino is lower right, and a global dataset of all the points of each of the six cities put on a single graph is at the bottom.

4.1.1.3. Fine Mode

Figure 9 presents the aggregated Sentinel-3a AOD and corresponding PM_{2.5} concentrations for the fine mode AOD wavelength band. The global graph, just like the previous global graphs, has the majority of points distributed in the lower left corner. There is an R^2 value of 0.1499, a slope of 52.358 and an intercept of 9.1559. The R^2 continues to vary massively between the different cities. Los Angeles has the highest correlation coefficient here, with an R^2 value of 0.3712, a slope of 45.424 and an intercept of 6.2636. On the other hand, Beijing has the lowest R^2 value of 0.004, a slope of -1.8154 and an intercept of 46.055.

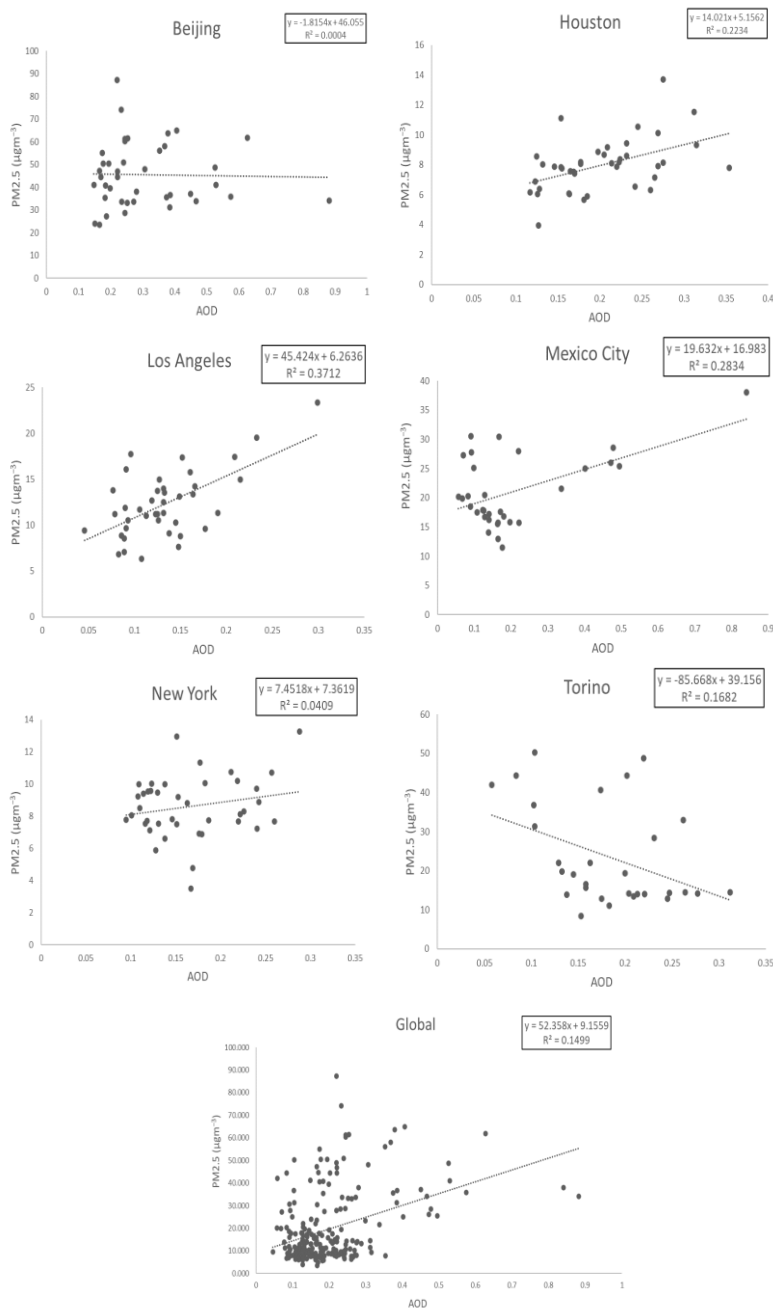


Figure 9: Linear relationship between Sentinel-3a AOD, using the Fine Mode wavelength band, and PM_{2.5} for a variety of cities. In order, Beijing is upper left, Houston is upper right, Los Angeles is middle left, Mexico City is middle right, New York

is lower left, Torino is lower right, and a global dataset of all the points of each of the six cities put on a single graph is at the bottom.

Finally, figure 10 presents the correlations between AERONET AOD and $PM_{2.5}$ for fine mode AOD. The global graph has an R^2 value of 0.4113, which is stronger than all of the cities presented. The second strongest correlation is found in Houston, with an R^2 value of 0.2483.

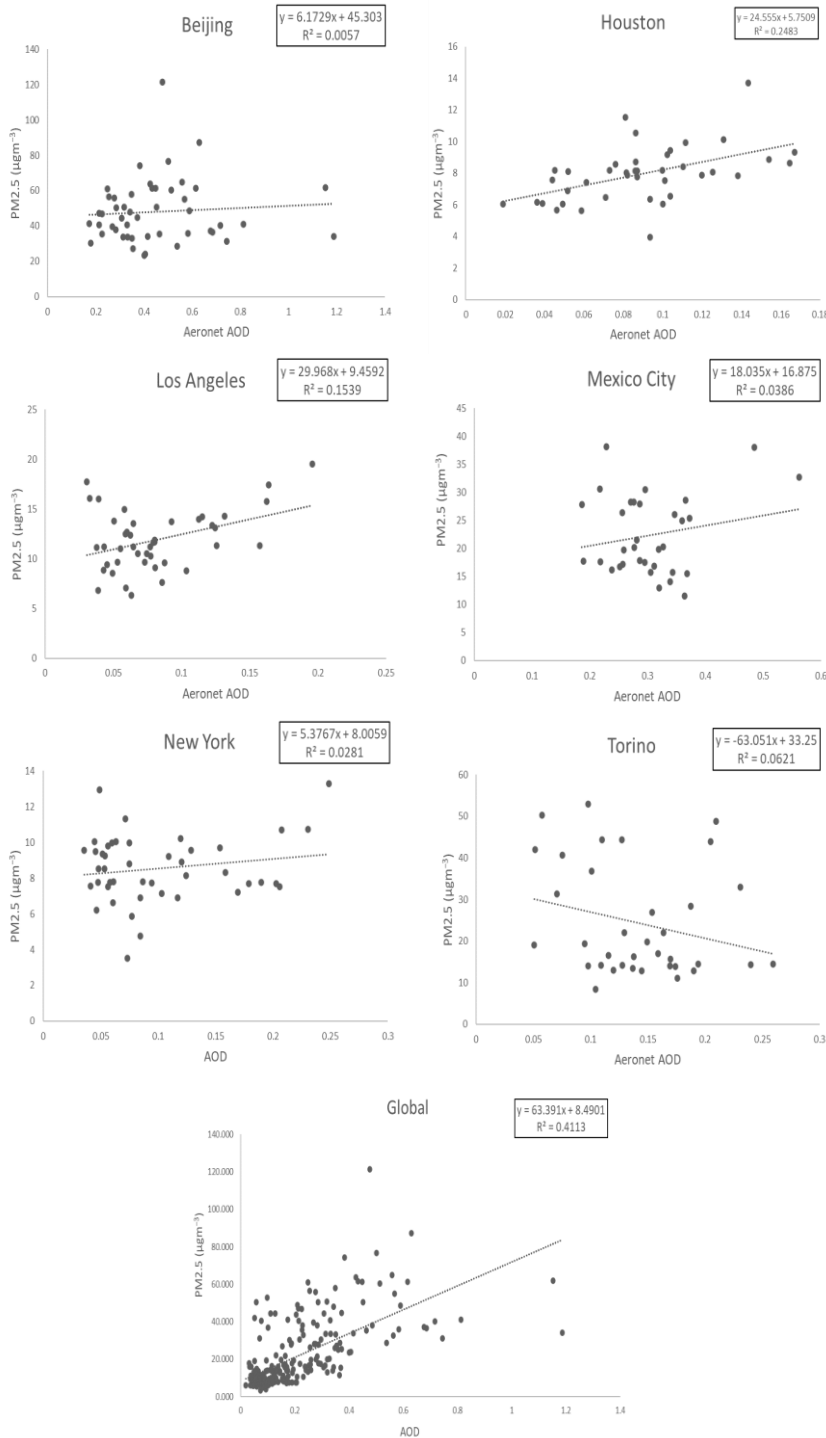


Figure 10: Linear relationship between Sentinel-3a AOD, using the Fine Mode wavelength band, and $PM_{2.5}$ for a variety of cities. In order, Beijing is upper left, Houston is upper right, Los Angeles is middle left, Mexico City is middle right, New York is lower left, Torino is lower right, and a global dataset of all the points of each of the six cities put on a single graph is at the bottom.

4.1.1.4 Comparison

Table 5 sums up the results of these graphs.

Table 11: Statistical Table showing the R^2 values, the slopes, and the intercepts for the six cities investigated. These are split between Sentinel-3a and AERONET

City	Instrument		R^2	Slope	Intercept
Beijing	Sentinel-3a	550nm	0.0273	-29.374	50.482
		870nm	0.0308	-31.141	50.927
		Fine Mode	0.0004	-1.8154	46.055
	AERONET	550nm	0.0233	14.347	40.86
		870nm	0.0293	26.56	40.333
		Fine Mode	0.0057	6.1729	45.303
Houston	Sentinel-3a	550nm	0.2726	13.039	4.9757
		870nm	0.3025	25.926	5.1216
		Fine Mode	0.2234	14.021	5.1562
	AERONET	550nm	0.5115	27.36	4.5042
		870nm	0.581	43.427	4.6462
		Fine Mode	0.2483	24.555	5.7509
Los Angeles	Sentinel-3a	550nm	0.1519	23.886	8.457
		870nm	0.2312	77.261	6.3461
		Fine Mode	0.3712	45.424	6.2636
	AERONET	550nm	0.0859	19.477	9.7485
		870nm	0.0464	23.925	10.284
		Fine Mode	0.1539	29.968	9.4592
Mexico City	Sentinel-3a	550nm	0.2779	20.7	16.247
		870nm	0.004	9.6846	20.032
		Fine Mode	0.2834	19.632	16.983
	AERONET	550nm	0.0457	18.836	17.809
		870nm	0.0025	12.068	20.641
		Fine Mode	0.0386	18.035	16.875
New York	Sentinel-3a	550nm	0.0284	6.2208	7.519
		870nm	0.0047	6.193	8.1545
		Fine Mode	0.0409	7.4518	7.3619
	AERONET	550nm	0.0177	4.6011	8.0147
		870nm	0.0084	6.3681	8.1851
		Fine Mode	0.0281	5.3767	8.0059
Torino	Sentinel-3a	550nm	0.2848	-94.714	43.981
		870nm	0.3734	-197.54	45.025
		Fine Mode	0.1682	-85.668	39.156
	AERONET	550nm	0.2356	-96.026	41.06
		870nm	0.2093	-179.18	39.623
		Fine Mode	0.0621	-63.051	33.25

In terms of performance, Sentinel-3a seems to perform at a similar level to AERONET. AERONET, on average, outperforms Sentinel-3a in Houston, with R^2 values of 0.5115, 0.581 and 0.2483 for 550nm,

870nm and fine mode AOD respectively, compared to Sentinel-3a's R^2 values of 0.2726, 0.3025, and 0.2234. However, Sentinel-3a outperforms AERONET in Los Angeles, with R^2 values of 0.1519, 0.2312, and 0.3712, compared to AERONET's 0.0859, 0.0464 and 0.1539, for 550nm, 870nm and fine mode AOD respectively. For each city, the performance of the correlation varied massively. This suggests that there is likely a lot more factors in play here that should have been corrected for. One such variable could be meteorological factors such as relative humidity or boundary layer height.

In order to test out if daily aggregation would have a significant impact on the correlation, instead of the monthly aggregation, a daily aggregation was made for Beijing and a linear regression graph was created for both Sentinel-3a and AERONET AOD. The R^2 values, slope and intercepts for both the daily and monthly correlations of Beijing are presented in table 6.

Table 12: Daily vs Monthly aggregation and statistics

City	Instrument	Timeseries	R^2	Slope	Intercept
Beijing	Sentinel-3a	Daily	0.0859	40.783	37.315
		Monthly	0.0273	-29.374	50.482
	AERONET	Daily	0.3681	44.986	29.132
		Monthly	0.0233	14.347	40.86

What is noticeable is the immediate increase in R^2 for both Sentinel-3a and AERONET, with the R^2 going up from 0.0273 to 0.0859 with Sentinel-3a and from 0.0233 to 0.3681 with AERONET. An interesting factor here is that the AERONET correlation increased a lot more than the Sentinel-3a dataset. This is likely since AERONET is ground based. As AERONET is gathering AOD data closer to the ground, where $PM_{2.5}$ datasets are measured, not only are meteorological conditions likely very similar, but there is no estimation of the AOD present in the atmospheric column, and rather the surface AOD. It is likely that Sentinel-3a AOD will need corrections.

5. Discussion

Overall, the results presented show that it is indeed possible to correlate Sentinel-3a AOD with ground-measured PM_{2.5}. However, the correlations presented in this study are too low to be suitable for deriving PM_{2.5} concentrations. This is most likely due to the coarse resolution of the AOD datasets, as it does not allow for the city-wide variability of data between each station to be shown. Additionally, aggregating the data monthly and not daily means that temporal variability is retracted from the dataset. Higher PM_{2.5} values between the stations because of the presence of industrial factories, or naturally elevated AOD datasets due to the background dust levels, will all be aggregated out to their averages with how it was conducted in this study. In future, a higher spatial resolution dataset with daily data should be considered.

6. Conclusions

Looking at the R^2 values of both the Sentinel-3a AOD and AERONET AOD, there is a similar performance in how the correlation works. For the 2017-2020 period, there are decent correlations between Sentinel-3a and $PM_{2.5}$, which is promising. The best R^2 created from Sentinel-3a is the 870nm Torino study at 0.3734, with the fine mode AOD for Los Angeles not far behind at 0.3712. However, when the Beijing daily aggregate correlation was presented, AERONET correlations outperformed Sentinel-3a. Henceforth, it could be said that Sentinel-3a AOD has the potential to estimate $PM_{2.5}$, but further research needs to be done to determine the best approach.

Future studies in this area could do multiple things. Firstly, daily aggregating the data would be massively beneficial, as demonstrated by the Beijing table. With how the daily gridded Sentinel-3a AOD data was presented, and how Sentinel-3a surveys the planet, there is not daily coverage provided, and there appear to be points that are surveyed more than others. A future study could look to see if the daily aggregation has a big effect on correlation when a large timeseries is covered.

Another factor that future studies could consider is whether a city-scale project is the best approach for Sentinel-3a. Considering it was presented as a $1^\circ \times 1^\circ$ lat-long grid, that might not be suitable for a high-resolution study such as a city-scale. It became apparent during this thesis as one grid on Sentinel-3a would correspond to tens of $PM_{2.5}$ stations, making it difficult to aggregate as to get a truer reflection of the atmospheric column, the $PM_{2.5}$ across the city needed to be averaged. Future studies could look at how Sentinel-3a performs at a country-scale $PM_{2.5}$ correlation, to see if that would be more suitable.

Finally, other meteorological parameters should have been accounted for in the study, to correct for relative humidity etc.

This study, whilst using smaller datasets due to the amount of aggregation, shows some promising results. Whilst the correlation between Sentinel-3a AOD and $PM_{2.5}$ could be improved, especially when compared against the robust AERONET AOD dataset, it does show that there is indeed a relationship between Sentinel-3a AOD and $PM_{2.5}$, which future studies can use.

Bibliography

Acharya, P. *et al.* (2021) 'Revisiting the levels of Aerosol Optical Depth in south-southeast Asia, Europe and USA amid the COVID-19 pandemic using satellite observations', *Environmental Research*, 193, p. 110514. doi:10.1016/J.ENVRES.2020.110514.

Bauer, S.E., Tsigaridis, K. and Miller, R. (2016) 'Significant atmospheric aerosol pollution caused by world food cultivation', *Geophysical Research Letters*, 43(10), pp. 5394–5400. doi:10.1002/2016GL068354.

Bian, H. *et al.* (2009) 'Sensitivity of aerosol optical thickness and aerosol direct radiative effect to relative humidity', *Atmospheric Chemistry and Physics*, 9(7), pp. 2375–2386. doi:10.5194/ACP-9-2375-2009.

Brook, R.D. *et al.* (2008) 'The Relationship Between Diabetes Mellitus and Traffic-Related Air Pollution', *Journal of Occupational & Environmental Medicine*, 50(1), pp. 32–38. doi:10.1097/JOM.0b013e31815dba70.

Buonanno, G. *et al.* (2015) 'Lung cancer risk of airborne particles for Italian population', *Environmental Research*, 142, pp. 443–451. doi:10.1016/J.ENVRES.2015.07.019.

Burnett, R.T. *et al.* (2014) 'An Integrated Risk Function for Estimating the Global Burden of Disease Attributable to Ambient Fine Particulate Matter Exposure', *Environmental Health Perspectives*, 122(4), pp. 397–403. doi:10.1289/EHP.1307049.

Carvour, M.L. *et al.* (2018) 'Estimating the Health and Economic Impacts of Changes in Local Air Quality', *American journal of public health*, 108(S2), pp. S151–S157. doi:10.2105/AJPH.2017.304252.

Chen, S. and Bloom, D.E. (2019) 'The macroeconomic burden of noncommunicable diseases associated with air pollution in China', *PLOS ONE*, 14(4), p. e0215663. doi:10.1371/JOURNAL.PONE.0215663.

Chiacchio, M. *et al.* (2011) 'Decadal variability of aerosol optical depth in Europe and its relationship to the temporal shift of the North Atlantic Oscillation in the realm of dimming and brightening', *Journal of Geophysical Research: Atmospheres*, 116(D2). doi:10.1029/2010JD014471.

CHRISTOPHER J. PACIOREK *et al.* (2008) 'Spatiotemporal Associations between GOES Aerosol Optical Depth Retrievals and Ground-Level PM 2.5', *Environ. Sci. Technol*, 42, pp. 5800–5806. doi:10.1021/es703181j.

Cohen, G. *et al.* (2019) 'Decoupling of emissions and GDP: Evidence from aggregate and provincial Chinese data', *Energy Economics*, 77, pp. 105–118. doi:10.1016/J.ENERCO.2018.03.030.

Conticini, E., Frediani, B. and Caro, D. (2020) 'Can atmospheric pollution be considered a co-factor in extremely high level of SARS-CoV-2 lethality in Northern Italy?', *Environmental Pollution*, 261, p. 114465. doi:10.1016/J.ENVPOL.2020.114465.

Danish *et al.* (2018) 'The effect of ICT on CO2 emissions in emerging economies: does the level of income matters?', *Environmental Science and Pollution Research*, 25(23), pp. 22850–22860. doi:10.1007/S11356-018-2379-2/TABLES/5.

van Donkelaar, A., Martin, R. v. and Park, R.J. (2006) 'Estimating ground-level PM2.5 using aerosol optical depth determined from satellite remote sensing', *Journal of Geophysical Research: Atmospheres*, 111(D21), p. 21201. doi:10.1029/2005JD006996.

- Donlon, C. *et al.* (2012) 'The Global Monitoring for Environment and Security (GMES) sentinel-3 mission', *Remote Sensing of Environment*, 120, pp. 37–57. doi:10.1016/j.rse.2011.07.024.
- Dubovik, O. *et al.* (2019) 'Polarimetric remote sensing of atmospheric aerosols: Instruments, methodologies, results, and perspectives', *Journal of Quantitative Spectroscopy and Radiative Transfer*, 224, pp. 474–511. doi:10.1016/J.JQSRT.2018.11.024.
- Dutheil, F., Baker, J.S. and Navel, V. (2020) 'COVID-19 as a factor influencing air pollution?', *Environmental Pollution*, 263, p. 114466. doi:10.1016/J.ENVPOL.2020.114466.
- Dyer, C. (2020) 'Air pollution from road traffic contributed to girl's death from asthma, coroner concludes', *BMJ*, 371, p. m4902. doi:10.1136/BMJ.M4902.
- Environmental Protection Agency (EPA) (2013) *Federal Register :: National Ambient Air Quality Standards for Particulate Matter*. Available at: <https://www.federalregister.gov/documents/2013/01/15/2012-30946/national-ambient-air-quality-standards-for-particulate-matter> (Accessed: 30 September 2022).
- Feng, K. *et al.* (2013) 'Outsourcing CO₂ within China', *Proceedings of the National Academy of Sciences of the United States of America*, 110(28), pp. 11654–11659. doi:10.1073/PNAS.1219918110/SUPPL_FILE/PNAS.201219918SI.PDF.
- Filonchyk, M. *et al.* (2019) 'Combined use of satellite and surface observations to study aerosol optical depth in different regions of China', *Scientific Reports 2019 9:1*, 9(1), pp. 1–15. doi:10.1038/s41598-019-42466-6.
- Filonchyk, M. *et al.* (2020) 'Impact Assessment of COVID-19 on Variations of SO₂, NO₂, CO and AOD over East China', *Aerosol and Air Quality Research*, 20(7), pp. 1530–1540. doi:10.4209/AAQR.2020.05.0226.
- Freire, C. *et al.* (2010) 'Association of traffic-related air pollution with cognitive development in children', *Journal of Epidemiology & Community Health*, 64(3), pp. 223–228. doi:10.1136/jech.2008.084574.
- Giannakis, E. *et al.* (2019) 'Exploring the economy-wide effects of agriculture on air quality and health: Evidence from Europe', *Science of The Total Environment*, 663, pp. 889–900. doi:10.1016/J.SCITOTENV.2019.01.410.
- Graber, E.R. and Rudich, Y. (2006) 'Atmospheric HULIS: How humic-like are they? A comprehensive and critical review', *Atmospheric Chemistry and Physics*, 6(3), pp. 729–753. doi:10.5194/ACP-6-729-2006.
- Huang, J. *et al.* (2018) 'Health impact of China's Air Pollution Prevention and Control Action Plan: an analysis of national air quality monitoring and mortality data', *The Lancet Planetary Health*, 2(7), pp. e313–e323. doi:10.1016/S2542-5196(18)30141-4.
- Im, U. *et al.* (2018) 'Assessment and economic valuation of air pollution impacts on human health over Europe and the United States as calculated by a multi-model ensemble in the framework of AQMEII3', *Atmospheric Chemistry and Physics*, 18(8), pp. 5967–5989. doi:10.5194/acp-18-5967-2018.
- Jain, S. and Sharma, T. (2020) 'Social and Travel Lockdown Impact Considering Coronavirus Disease (COVID-19) on Air Quality in Megacities of India: Present Benefits, Future Challenges and Way Forward', *Aerosol and Air Quality Research*, 20(6), pp. 1222–1236. doi:10.4209/AAQR.2020.04.0171.

- Kan, H. and Chen, B. (2004) 'Particulate air pollution in urban areas of Shanghai, China: health-based economic assessment', *Science of The Total Environment*, 322(1–3), pp. 71–79. doi:10.1016/J.SCITOTENV.2003.09.010.
- Kaskaoutis, D.G. *et al.* (2010) 'Aerosol Monitoring over Athens Using Satellite and Ground-Based Measurements', *Advances in Meteorology*, 2010, pp. 1–12. doi:10.1155/2010/147910.
- Kim, D. *et al.* (2019) 'Estimation of health benefits from air quality improvement using the MODIS AOD dataset in Seoul, Korea', *Environmental Research*, 173, pp. 452–461. doi:10.1016/J.ENVRES.2019.03.042.
- Kong, L. *et al.* (2016) 'The empirical correlations between PM_{2.5}, PM₁₀ and AOD in the Beijing metropolitan region and the PM_{2.5}, PM₁₀ distributions retrieved by MODIS', *Environmental Pollution*, 216, pp. 350–360. doi:10.1016/J.ENVPOL.2016.05.085.
- Kumar, A., Saxena, D. and Yadav, R. (2011) 'Measurements of atmospheric aerosol concentration of various sizes during monsoon season at Roorkee, India', *Atmospheric Science Letters*, 12(4), pp. 345–350. doi:10.1002/ASL.347.
- Kumar, N., Chu, A. and Foster, A. (2007) 'An empirical relationship between PM_{2.5} and aerosol optical depth in Delhi Metropolitan', *Atmospheric environment (Oxford, England : 1994)*, 41(21), p. 4492. doi:10.1016/J.ATMOSENV.2007.01.046.
- de la Campa, A.M.S. and de la Rosa, J.D. (2014) 'Implications for air quality and the impact of financial and economic crisis in South Spain: Geochemical evolution of atmospheric aerosol in the ceramic region of Bailén', *Atmospheric Environment*, 98, pp. 519–529. doi:10.1016/J.ATMOSENV.2014.09.023.
- Lalitaporn, P. and Mekaumnuaychai, T. (2020) 'Satellite measurements of aerosol optical depth and carbon monoxide and comparison with ground data', *Environmental Monitoring and Assessment*, 192(6), pp. 1–19. doi:10.1007/S10661-020-08346-7/FIGURES/9.
- Lee, C.J. *et al.* (2015) 'Response of Global Particulate-Matter-Related Mortality to Changes in Local Precursor Emissions'. doi:10.1021/acs.est.5b00873.
- Lelieveld, J. *et al.* (2015) 'The contribution of outdoor air pollution sources to premature mortality on a global scale', *Nature* 2015 525:7569, 525(7569), pp. 367–371. doi:10.1038/nature15371.
- Levy, H. *et al.* (2013) 'The roles of aerosol direct and indirect effects in past and future climate change', *Journal of Geophysical Research: Atmospheres*, 118(10), pp. 4521–4532. doi:10.1002/JGRD.50192.
- Lim, S. *et al.* (2022) 'Comparing human exposure to fine particulate matter in low and high-income countries: A systematic review of studies measuring personal PM_{2.5} exposure', *Science of The Total Environment*, 833, p. 155207. doi:10.1016/J.SCITOTENV.2022.155207.
- Liu, C. *et al.* (2019) 'The impacts of economic restructuring and technology upgrade on air quality and human health in Beijing-Tianjin-Hebei region in China', *Frontiers of Environmental Science and Engineering*, 13(5). doi:10.1007/S11783-019-1155-Y.
- Longhurst, J. *et al.* (2018) 'ANALYSING AIR POLLUTION AND ITS MANAGEMENT THROUGH THE LENS OF THE UN SUSTAINABLE DEVELOPMENT GOALS: A REVIEW AND ASSESSMENT'. doi:10.2495/AIR180011.

- Loomis, D. *et al.* (2013) 'The carcinogenicity of outdoor air pollution', *The Lancet Oncology*, 14(13), pp. 1262–1263. doi:10.1016/S1470-2045(13)70487-X.
- Ma, X., Ge, R. and Zhang, L. (2014) 'Research on the relationship between air quality and economy development in major cities of China', *Kybernetes*. Edited by D. Mourad Oussalah and Professor Ali Hessami, 43(8), pp. 1224–1236. doi:10.1108/K-07-2013-0146.
- McMurry, P.H. *et al.* (no date) 'Particulate Matter Science for Policy Makers A NARSTO Assessment'. Available at: www.cambridge.org (Accessed: 17 September 2023).
- Meier, J. *et al.* (2012) 'A regional model of European aerosol transport: Evaluation with sun photometer, lidar and air quality data', *Atmospheric Environment*, 47, pp. 519–532. doi:10.1016/J.ATMOENV.2011.09.029.
- de Meij, A., Pozzer, A. and Lelieveld, J. (2012) 'Trend analysis in aerosol optical depths and pollutant emission estimates between 2000 and 2009', *Atmospheric Environment*, 51, pp. 75–85. doi:10.1016/J.ATMOENV.2012.01.059.
- Mi, Z.F. *et al.* (2015) 'Potential impacts of industrial structure on energy consumption and CO2 emission: a case study of Beijing', *Journal of Cleaner Production*, 103, pp. 455–462. doi:10.1016/J.JCLEPRO.2014.06.011.
- Mishchenko, M.I. and Geogdzhayev, I. v. (2007) 'Satellite remote sensing reveals regional tropospheric aerosol trends', *Optics Express*, 15(12), p. 7423. doi:10.1364/OE.15.007423.
- Mishchenko, M.I., Travis, L.D. and Lacis, A.A. (2002) *Scattering, absorption, and emission of light by small particles*. Cambridge University Press.
- Munir, K. and Ameer, A. (2018) 'Effect of economic growth, trade openness, urbanization, and technology on environment of Asian emerging economies', *Management of Environmental Quality: An International Journal*, 29(6), pp. 1123–1134. doi:10.1108/MEQ-05-2018-0087.
- Nyeki, S. *et al.* (2012) 'Ground-based aerosol optical depth trends at three high-altitude sites in Switzerland and southern Germany from 1995 to 2010', *Journal of Geophysical Research: Atmospheres*, 117(D18), p. 18202. doi:10.1029/2012JD017493.
- Ortiz, C. *et al.* (2017) 'Evaluation of short-term mortality attributable to particulate matter pollution in Spain', *Environmental Pollution*, 224, pp. 541–551. doi:10.1016/J.ENVPOL.2017.02.037.
- Palancar, G.G. *et al.* (2013) 'Effect of aerosols and NO2 concentration on ultraviolet actinic flux near Mexico City during MILAGRO: Measurements and model calculations', *Atmospheric Chemistry and Physics*, 13(2), pp. 1011–1022. doi:10.5194/ACP-13-1011-2013.
- Petelski, T. *et al.* (2014) 'Studies of vertical coarse aerosol fluxes in the boundary layer over the Baltic Sea', *Oceanologia*, 56(4), pp. 697–710. doi:10.5697/OC.56-4.697.
- Peters, A. *et al.* (2001) 'Particulate air pollution is associated with an acute phase response in men Results from the MONICA-Augsburg Study', *European Heart Journal*, 22, pp. 1198–1204. doi:10.1053/euhj.2000.2483.
- Phalen, R.F. and Phalen., R.N. (2013) 'Introduction to Air Pollution Science: A Public Health Perspective', *Jones & Bartlett Learning, LLC*, pp. 21–40. Available at: https://books.google.com/books/about/Introduction_to_Air_Pollution_Science.html?id=2TGqgEY4WsMC (Accessed: 30 September 2022).

Pueschel, R. (1995) 'Atmospheric Aerosols', in Singh, H. (ed.) *Composition, chemistry, and climate of the atmosphere*, pp. 120–175.

Sahu, S.K. *et al.* (2020) 'The impact of aerosol direct radiative effects on PM_{2.5}-related health risk in Northern Hemisphere during 2013–2017', *Chemosphere*, 254, p. 126832. doi:10.1016/J.CHEMOSPHERE.2020.126832.

Schneider, R. *et al.* (2020) 'A Satellite-Based Spatio-Temporal Machine Learning Model to Reconstruct Daily PM_{2.5} Concentrations across Great Britain', *Remote Sensing*, 12(22), p. 3803. doi:10.3390/rs12223803.

Sheel, V., Guleria, R.P. and Ramachandran, S. (2018) 'Global and regional evaluation of a global model simulated AODs with AERONET and MODIS observations', *International Journal of Climatology*, 38, pp. e269–e289. doi:10.1002/JOC.5367.

Shi, Y. *et al.* (2018) 'Improving satellite aerosol optical Depth-PM_{2.5} correlations using land use regression with microscale geographic predictors in a high-density urban context', *Atmospheric Environment*, 190, pp. 23–34. doi:10.1016/J.ATMOENV.2018.07.021.

Strandgren, J. *et al.* (2014) 'Satellite retrieved AOD spatial resolution effect on PM 2.5 prediction Study of satellite retrieved aerosol optical depth spatial resolution effect on particulate matter concentration prediction Satellite retrieved AOD spatial resolution effect on PM 2.5 prediction Satellite retrieved AOD spatial resolution effect on PM 2.5 prediction', *Atmos. Chem. Phys. Discuss*, 14, pp. 25869–25899. doi:10.5194/acpd-14-25869-2014.

Svensden, E.R. *et al.* (no date) 'Circulating neutrophil CD14 expression and the inverse association of ambient particulate matter on lung function in asthmatic children'.

Tarín-Carrasco, P. *et al.* (2019) 'Isolating the climate change impacts on air-pollution-related-pathologies over central and southern Europe – a modelling approach on cases and costs', *Atmospheric Chemistry and Physics*, 19(14), pp. 9385–9398. doi:10.5194/acp-19-9385-2019.

'The National Ambient Air Quality Standards for Particle Pollution REVISED AIR QUALITY STANDARDS FOR PARTICLE POLLUTION AND UPDATES TO THE AIR QUALITY INDEX (AQI)' (no date).

Tian, J. and Chen, D.M. (2007) 'Evaluating satellite-based measurements for mapping air quality in Ontario, Canada', *Journal of Environmental Informatics*, 10(1), pp. 30–36. doi:10.3808/JEI.200700097.

Torres, O. *et al.* (2007) 'Aerosols and surface UV products from Ozone Monitoring Instrument observations: An overview', *Journal of Geophysical Research: Atmospheres*, 112(D24), pp. 24–47. doi:10.1029/2007JD008809.

UNICEF (2016) *Clean the Air for Children*. Available at: https://www.unicef.org/media/49966/file/UNICEF_Clear_the_Air_for_Children_30_Oct_2016.pdf (Accessed: 30 September 2022).

Visbeck, M. (2018) 'Ocean science research is key for a sustainable future', *Nature Communications* 2018 9:1, 9(1), pp. 1–4. doi:10.1038/s41467-018-03158-3.

Wallace, J.M. and Hobbs, P. v. (2006) 'Atmospheric Science: An Introductory Survey: Second Edition', *Atmospheric Science: An Introductory Survey: Second Edition*, pp. 1–488. doi:10.1016/C2009-0-00034-8.

- Wang, J. and Christopher, S.A. (2003) 'Intercomparison between satellite-derived aerosol optical thickness and PM_{2.5} mass: Implications for air quality studies', *Geophysical Research Letters*, 30(21), p. 2095. doi:10.1029/2003GL018174.
- Wang, Pengfei *et al.* (2020) 'Severe air pollution events not avoided by reduced anthropogenic activities during COVID-19 outbreak', *Resources, Conservation and Recycling*, 158, p. 104814. doi:10.1016/J.RESCONREC.2020.104814.
- Wang, Q. *et al.* (2019) 'Impacts of short-Term mitigation measures on PM_{2.5} and radiative effects: A case study at a regional background site near Beijing, China', *Atmospheric Chemistry and Physics*, 19(3), pp. 1881–1899. doi:10.5194/ACP-19-1881-2019.
- Wei, X. *et al.* (2020) 'Satellite remote sensing of aerosol optical depth: advances, challenges, and perspectives', *Critical Reviews in Environmental Science and Technology*, 50(16), pp. 1640–1725. doi:10.1080/10643389.2019.1665944.
- Xin, J. *et al.* (2014) 'The empirical relationship between the PM_{2.5} concentration and aerosol optical depth over the background of North China from 2009 to 2011', *Atmospheric Research*, 138, pp. 179–188. doi:10.1016/J.ATMOSRES.2013.11.001.
- Xin, J. *et al.* (2016) 'The observation-based relationships between PM_{2.5} and AOD over China', *Journal of Geophysical Research: Atmospheres*, 121(18), pp. 10,701-10,716. doi:10.1002/2015JD024655.
- Xu, Q. *et al.* (2021) 'Spatiotemporal relationship between Himawari-8 hourly columnar aerosol optical depth (AOD) and ground-level PM_{2.5} mass concentration in mainland China', *Science of The Total Environment*, 765, p. 144241. doi:10.1016/J.SCITOTENV.2020.144241.
- Xue, Y. *et al.* (2014) 'China Collection 2.0: The aerosol optical depth dataset from the synergetic retrieval of aerosol properties algorithm', *Atmospheric Environment*, 95, pp. 45–58. doi:10.1016/J.ATMOENV.2014.06.019.
- Xue, Y. *et al.* (2017) 'Long-time series aerosol optical depth retrieval from AVHRR data over land in North China and Central Europe', *Remote Sensing of Environment*, 198, pp. 471–489. doi:10.1016/J.RSE.2017.06.036.
- Yang, Q. *et al.* (2019) 'The relationships between PM_{2.5} and aerosol optical depth (AOD) in mainland China: About and behind the spatio-temporal variations', *Environmental Pollution*, 248, pp. 526–535. doi:10.1016/J.ENVPOL.2019.02.071.
- Yang, Y. *et al.* (2020) 'Impacts of aerosol-radiation interaction on meteorological forecasts over northern China by offline coupling of the WRF-Chem-simulated aerosol optical depth into WRF: A case study during a heavy pollution event', *Atmospheric Chemistry and Physics*, 20(21), pp. 12527–12547. doi:10.5194/ACP-20-12527-2020.
- Yao, F. *et al.* (2018) 'A multidimensional comparison between MODIS and VIIRS AOD in estimating ground-level PM_{2.5} concentrations over a heavily polluted region in China', *Science of The Total Environment*, 618, pp. 819–828. doi:10.1016/J.SCITOTENV.2017.08.209.
- Yin, X. *et al.* (2019) 'Gaseous and particulate pollutants in Lhasa, Tibet during 2013–2017: Spatial variability, temporal variations and implications', *Environmental Pollution*, 253, pp. 68–77. doi:10.1016/J.ENVPOL.2019.06.113.

Zhang, Y. and Li, Z. (2015) 'Remote sensing of atmospheric fine particulate matter (PM2.5) mass concentration near the ground from satellite observation', *Remote Sensing of Environment*, 160, pp. 252–262. doi:10.1016/J.RSE.2015.02.005.

Zhang, Y., Wen, X.Y. and Jang, C.J. (2010) 'Simulating chemistry–aerosol–cloud–radiation–climate feedbacks over the continental U.S. using the online-coupled Weather Research Forecasting Model with chemistry (WRF/Chem)', *Atmospheric Environment*, 44(29), pp. 3568–3582. doi:10.1016/J.ATMOSENV.2010.05.056.

Zheng, C. *et al.* (2017) 'Analysis of influential factors for the relationship between PM2.5 and AOD in Beijing', *Atmospheric Chemistry and Physics*, 17(21), pp. 13473–13489. doi:10.5194/ACP-17-13473-2017.

Zhou, M. *et al.* (2015) 'Smog episodes, fine particulate pollution and mortality in China', *Environmental research*, 136, pp. 396–404. doi:10.1016/J.ENVRES.2014.09.038.

Zielinski, T. *et al.* (2016) 'Impact of wild forest fires in Eastern Europe on aerosol composition and particle optical properties', *Oceanologia*, 58(1), pp. 13–24. doi:10.1016/j.oceano.2015.07.005.